Meta-Analysis and Structural Dynamics of the Emergence of Genetic Variants of SARS-CoV-2

Nicolas Castonguay[1], Wandong Zhang[2,3] and Marc-Andre Langlois[1,4*]

[1]Department of Biochemistry, Microbiology & Immunology, Faculty of Medicine, University of Ottawa, Ontario, Canada K1H 8M5.

[2]Department of Cellular & Molecular Medicine, Faculty of Medicine, University of Ottawa, Ontario, Canada K1H 8M5.

[3]Human Health Therapeutics Research Centre, National Research Council Canada, Ottawa, Canada K1A 0R6

[4]uOttawa Center for Infection, Immunity and Inflammation (CI3).

Running title: **Genome Evolution of SARS-CoV-2.**

*Correspondence should be addressed to: langlois@uottawa.ca

Key words: SARS-CoV-2, COVID-19, Variants of concern, B.1.1.7, B1.351, P.1, D614G

ABSTRACT

The novel Severe Acute Respiratory Syndrome Coronavirus 2 (SARS-CoV-2) emerged in late December 2019 in Wuhan, China, and is the causative agent for the worldwide COVID-19 pandemic. SARS-CoV-2 is a positive-sense single-stranded RNA virus belonging to the betacoronavirus genus. Due to the error-prone nature of the viral RNA-dependent polymerase complex, coronaviruses are known to acquire new mutations at each cycle of genome replication. This constitutes one of the main factors driving the evolution of its relatively large genome and the emergence of new genetic variants. In the past few months, the identification of new B.1.1.7 (UK), B.1.351 (South Africa) and P.1 (Brazil) variants of concern (VOC) have highlighted the importance of tracking the emergence of mutations in the SARS-CoV-2 genome that impact transmissibility, virulence, and immune and neutralizing antibody escape. Here we analyzed the appearance and prevalence trajectory over time of mutations that appeared in all SARS-CoV-2 genes from December, 2019 to April, 2021. The goal of the study was to identify which genetic modifications are the most frequent and study the dynamics of their propagation, their incorporation into the consensus sequence, and their impact on virus biology. We also analyzed the structural properties of the spike glycoprotein of the B.1.1.7, B.1.351 and P.1 variants for its binding to the host receptor ACE2. This study offers an integrative view of the emergence, disappearance, and consensus sequence integration of successful mutations that constitute new SARS-CoV-2 variants and their impact on neutralizing antibody therapeutics and vaccines.

IMPORTANCE

SARS-CoV-2 is the etiological agent of COVID-19, which has caused > 3.4 million deaths worldwide as of April, 2021. Mutations occur in the genome of SARS-CoV-2 during viral replication and affect viral infectivity, transmissibility, and virulence. In early March 2020, the D614G mutation in the spike protein emerged, which increased viral transmissibility and is now found in over 90% of all SARS-CoV-2 genomic sequences in GISAID database. Between October and December 2020, B.1.1.7 (UK), B.1.351 (South Africa) and P.1 (Brazil) variants of concern (VOCs) emerged, which have increased neutralizing antibody escape capabilities because of mutations in the receptor binding domain of the spike protein. Characterizing mutations in these variants is crucial because of their effect on adaptive immune responses, neutralizing antibody therapy, and their impact on vaccine efficacy. Here we tracked and analyzed mutations in SARS-CoV-2 genes since the beginning of the pandemic and investigated their functional impact on the spike of these three VOCs.

Graphical Abstract

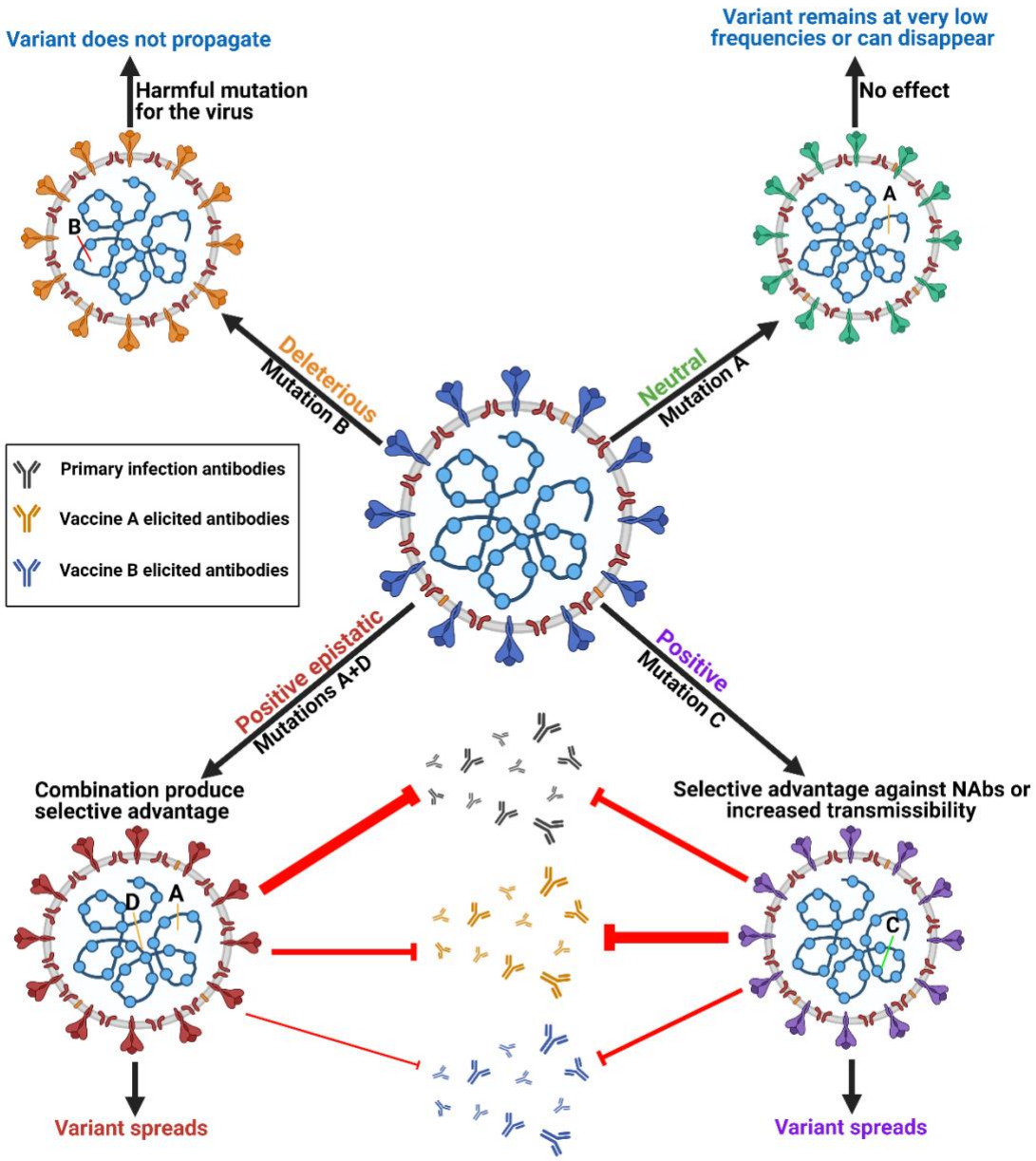

INTRODUCTION

In late December 2019, a new betacoronavirus known as Severe Acute Respiratory Syndrome Coronavirus 2 (SARS-COV-2) emerged in the city of Wuhan in the province of Hubei, China (1). SARS-CoV-2 is the etiological viral agent for the worldwide COVID-19 pandemic resulting in more than 162 million infected and 3.4 million deaths worldwide as of April, 2021 (2,3). SARS-CoV-2 is an enveloped, positive-sense single-stranded RNA (+ssRNA) virus with a genome length of 29,811 nucleotides (4). The mutation rates of RNA viruses are generally higher than that of DNA viruses because of the low fidelity of their viral RNA polymerases (5,6). Mutations occur when viral replication enzymes introduce errors in the viral genome resulting in the creation of premature termination codons, deletions and insertions of nucleotides that can alter open reading frames and result in amino acid substitutions in viral proteins. These mutations combined with the selective pressure of the human immune system lead to the selection and evolution of viral genomes (6,7). However, coronaviruses are one of the few members of the RNA virus family that possess limited but measurable proofreading ability via the 3'-to 5'- exoribonuclease activity of the non-structural viral protein 14 (nsp14) (8,9). Coronaviruses are therefore expected to evolve through genetic drift much slower than other RNA viruses that do not have this ability, such as influenza viruses (8,10). Additionally, SARS-CoV-2 and other coronaviruses have low known occurrences of recombination between family members (i.e., genetic shift), and therefore are mostly susceptible to genetic drift (11).

SARS-CoV-2 has reached pandemic status due to its presence on every continent and has since maintained a high level of transmissibility across hosts of various ethnical and genetic backgrounds (2, 12). Moreover, SARS-CoV-2 infections have been reported to naturally infect minks, ferrets, cats, tiger, and dogs, which allows the virus to replicate in completely new hosts and mutate to produce new variants and possibly new strains (13,14). In March 2020, the now dominant D614G mutation first emerged in the spike protein (S) of SARS-CoV-2. The S protein is present as a trimer at the surface of the viral envelope and is responsible for attachment of the virus to the human angiotensin converting enzyme 2 (hACE2), the entry receptor for SARS-CoV-2 into human cells (15). Published evidence has now shown that D614G increases viral fitness, transmissibility and viral load but does not directly affect COVID-19 pathogenicity (16,17,18,19). Additionally, emerging evidence indicates that D614G may have epistatic interactions that exacerbate the impact of several other independent mutations (19). Mutations in the S protein, and particularly in the receptor binding domain (RBD), are of very high concern given that they can directly influence viral infectivity, transmissibility, and resistance to neutralizing antibodies and T cell responses.

New mutations are frequently and regularly detected in the genome of SARS-CoV-2 through whole genome sequencing; however, very few of these mutations make it into the transmitted viral consensus sequence. The reference strain is generally regarded as the dominant transmitted strain at a given time. Its sequence

is determined by aligning large numbers of recently sequenced genomes and establishing a consensus sequence composed of the highest frequency nucleotide for each position in the viral genome. A genetic variant is a version of the reference strain that has acquire one or several new mutations and acts as the founder for further genetic diversification and evolution. Mutations arise regularly in the reference strain, but few are longitudinally conserved. Genetic variants are therefore the rare successful offshoots of the reference strain.

Some variants rise rapidly in frequency and then collapse and disappear, while others will rise and overtake the frequency of the reference strain and become the new reference. There are three main genetic variants that have emerged in the past few months with sustained upward frequency trajectories. The first is the UK variant, also known as B.1.1.7/501Y.V1 (B1.1.7). It was first detected in September 2020 and is now present worldwide and poised to become the new reference strain (20,21). The South African variant, also known as B.1.351/501Y.V2 (B.1.351), was first reported in October 2020 and is now increasing in prevalence in South Africa, Europe, and North America (21,22). The Brazilian variant, P.1/501Y.V3 (P.1), was first detected in travelers from Brazil that landed in Japan in January 2021 (23). It has since been identified in 42% of specimens in the Amazonian city of Manaus and in the U.S. at the end of January 2021 (23). These three variants are associated with increased resistance to neutralizing antibodies (Nabs) and all possess the N501Y mutation, which is a mutation in the RBD that is critical for the spike protein to interact with hACE2 (24,25,26). This mutation is reported to cause increased resistance to Nabs, increased transmissibility, and increased virulence in animal models (27). In addition to the N501Y mutation, both the South African and Brazil variants possesses RBD mutations K417N(T) and E484K, which are also associated with further increased Nabs escape capabilities (24,25).

Here we present a retrospective metadata analysis of mutations throughout the SARS-CoV-2 genome that reached at least a 1% worldwide frequency between December 2019 and January 2021. We specifically investigated their frequency trajectory over time and their fixation into the reference sequencing using the Global Initiative on Sharing Avian Influenza Data (GISAID) (28). Additionally, we analyzed mutations in the S protein of the B.1.1.7, B.1.351 and P.1 variants and illustrated their impact on molecular interactions between the S protein and hACE2 and their potential impact on Nabs.

MATERIALS AND METHODS

Data collection and mutational analysis

Genomes uploaded to the GISAID EpiCoV™ server database were analyzed from December 1st, 2019, to December 31st, 2020, and selected viral sequences with submission dates from December 1st, 2019 to January 6, 2021. We first selected recurring mutations that were present in more than 500 reported genomes by August 2020, and another selection was made in January 2021 to capture recurring mutations present in more than 4000 reported genomes in GISAID. This strategy allowed us to study mutations reaching at least 1% in worldwide frequency. We filtered through 309,962 genomes for the analysis of selected mutations.

The worldwide frequency of the hCoV-19/Wuhan strain, and hCoV-19/D614G, B.1.1.7, B.1.351, and P.1 variants were analyzed from December 1st, 2019 to April 30th 2021. For the analysis of the mutations in B.1.1.7, B.1.351, and P.1 variants, we used the GISAID EpiCoV™ server database. Viral sequences on GISAID with submission dates between December 1st, 2019 and April 30th 2021 were selected for the analysis. We filtered through 1,090,689 genomes for the analysis of the variants. Only complete SARS-CoV-2 genomes (28 to 30 Kbps) isolated from human hosts were analyzed. MUSCLE alignment tool on UGene, and SnapGene was used to determine the nucleotide mutations and codon changes of the non-synonymous and synonymous mutations by sequence alignments to the NCBI SARS-CoV-2 reference genome (NC_045512). All genomes uploaded to the GISAID database that were used in this study are presented in **Supplementary Table 1**. Graphs of mutations and variants were performed in RStudio with timelines, and genomes illustrations were produced in Biorender.

Structural modeling

Mutations in the spike protein in complex with hACE2 were analyzed using a mutagenesis tool for PyMOL (PDB: 7A94). Visualizations of mutations in the B.1.1.7, B.1.351 and P.1 variants were produced using the spike protein closed conformation (PDB: 6ZGE), interaction with hACE2 (PDB: 7A94), interaction with C102 Nab (PDB: 7K8M), and interaction with C121 Nab (PDB: 7K8X). Figures and rendering were prepared with PyMOL.

RESULTS

Identification of emerging mutations in various SARS-CoV-2 genes. Emerging mutations in the SARS-CoV-2 genome were investigated to illustrate the fluctuations of these mutations during a period of twelve months. We tracked genome mutations with a worldwide frequency greater than 1% from December 2019 to December 31st, 2020 in the GISAID database. Genes NSP8, NSP10, NS6, NS7a, and E are not illustrated in **Figure 1** given that they did not display mutations with frequencies sufficiently high to meet our inclusion criteria during the study period. This is indicative that these are some of the most conserved sequences of the SARS-CoV-2 genome. Viral proteins that have low mutation frequencies could be due to evolutionary constraints. Some of these viral proteins may be evolutionarily conserved and play important roles in virus assembly and stability, genome replication, and viral release from infected cells. Our analysis highlights the fixation of the D614G mutation in the S protein and that of the P323L mutation in the RNA-dependent RNA polymerase (RdRp) (**Fig.1**). These are the only mutations to have successfully become part of the reference sequence as of December 2020. They appeared to have emerged simultaneously in January, 2020 and became present in more than 90% of all sequenced genomes by June, 2020. Additionally, some other mutations also emerged rapidly but then stabilized in frequency or faded out. For example, Q57H (NS3), R203K (N), G204R (N) are mutations that emerged rapidly and appeared to have stabilized at a frequency of 15% to 40%. Others like I120F (NSP2), L37F (NSP6), S477N (S), and L84S (NS8) illustrate mutations that emerged rapidly and then faded-out just as quickly. We also demonstrate that most genes in SARS-CoV-2 have mutations with overall frequencies lower than 10% (**Fig.1)**. These mutations are also summarized into **Table 1**, which illustrates nucleotide substitution producing the amino acid change, the frequency, and their respective effects. Globally, there is an uneven effort to test for SARS-CoV-2 infections in the population and sequence the viral genomes in those infected. As a result, emerging mutations go unreported until they reach countries with more intensive sequencing capabilities. Therefore, mutations presented here vastly underrepresent the global landscape of mutation frequency dynamics.

Geographic localization and timeline of the viral genes with mutations higher than 50% frequency. We next turned our attention to viral genes where at least one mutation reached a frequency higher than 50%. Only three genes met this criterion: NSP12, S, and N. We then took their mutation graphs and added worldwide geographic data provided from GISAID. Geomaps are useful to determine if a mutation is a localized and regional event or is found worldwide. In the S protein, D614G is found worldwide with initially higher reported cases in the US, UK, and Australia, probably due to more intense large-scale testing and sequencing, while A222V is mostly reported in the UK, but has not yet been reported in South America, Central and East African regions (**Fig. 2A)**. Like D614G, P323L in the RdRp is also found worldwide, with higher reported cases in the US, UK, and Australia (**Fig. 2B)**. The N gene does not yet have successful

mutations that have attained reference sequence status, but R203K, G204R, A220V, D3L, and S235F all reached a frequency of 50% or higher during the study period. A220V emerged in August of 2020 and reached a frequency higher than 50% in October of 2020 (**Fig. 2D**). Mutations G204R, R203K and A220V in N gene are reported at high frequency in the UK, but were not been detected in South America, Central, East, and South African regions (**Fig. 2C)**. We also observe the emergence of several mutations in S and N present in the B.1.1.7 variant, which now have a frequency higher than 65% (**Fig. 2C, 2D and Table 2**). The analysis of these data illustrate the localization of the most prevalent mutations to date, which appear to be mostly present in Western high-income countries. This, however, is undoubtable attributable to overall more intense testing and sequencing.

Localization and molecular interactions of prevalent S protein mutations. Here we illustrate the molecular interactions and spatial localization of the mutations in the S protein. PyMOL was used to model structures of the S protein binding to ACE2 and we analyze the possible effects of specific mutations at given positions in the protein. **Figure 3A** presents an overview of the physical positions of S protein mutations. The A222V mutation has no reported effects on protein stability, neutralizing antibody escape, and affinity for hACE2 **(Table 1)**. The substitution from A to V results in a low steric clash between neighboring residues (**Fig. 3B)**. The S477N substitution in the RBD enables increased stability during hACE2-RBD interactions (**Fig. 3C, Table 1)**. In the N-terminal domain (NTD), mutation L18F leads to a steric clash between neighboring residues (**Fig. 3D)**. However, this does not appear to impact the stability of the protein given that no such effects have been reported so far (**Table 1)**. In the closed conformation, D614 makes an ionic bond with K854 in the S2 subunit of another S protein monomer (**Fig. 3F)** (29). In the open conformation, D614 (or G614) doesn't make interactions or display steric clashes with neighboring residues (**Fig. 3E)**.

The emergence of the B.1.1.7 variant in the UK. A new variant was discovered in late 2020 in the UK that displayed increased affinity to hACE2, virulence and Nabs escape capabilities (**Fig. 4**) (24,25,30,31). Here we further investigated the B.1.1.7 variant by looking at S protein mutations of this variant in complex with Nabs and hACE2. We mapped the localization of mutations with available Cryo-EM structures of the S protein and assessed the frequency of the variant by interrogating the GISAID database. There are nine mutations in the S protein out of the total 24 mutations in the B.1.1.7 SARS-CoV-2 genome (**Fig. 5A & 5E)**. Mutations in the S protein of the B.1.1.7 variant, except D614G, emerged in October of 2020 and reached a worldwide frequency of 70% to 80% in April 2021 (**Fig. 4, Fig. 5C, Table 2)**. N501Y, found in the RBD, can interact with K353 in hACE2 (**Fig. 5B & 5D, Fig. 8C)**. The N501Y mutation is associated with an increased affinity to hACE2, along with an increase in infectivity and virulence (**Table 2)**. **Figure 5G** illustrates the whole genome of SARS-CoV-2 with all nucleotide substitutions of the B.1.1.7 variant.

Substitutions C913T, C5986T, C14676T, C15279T, C16176T in ORF1ab, and T26801C in M protein are all synonymous mutations. Also, the C27972T mutation has a frequency of 75% and produces a premature stop codon in NS8 that inactivates the protein (Q27stop) without obvious consequences (**Fig. 5E, Table 2)** (32). These results allow us to better understand the frequencies, localization, and interactions of mutations in the S protein of the B.1.1.7 variant. For viruses, both synonymous and non-synonymous mutations are of importance. Synonymous mutations that don't change the amino acid sequence of proteins can still exercise very important functions. They can play a key role in docking sites for RNA binding proteins, transcription factors and primers, or partake in important secondary structures of the viral RNA like functional loops and folds.

The emergence of the B.1.351 variant in South Africa. During the spread of the B.1.1.7 variant in the UK, another variant was emerging in South Africa, known as B.1.351 (21,22). The GISAID database was used to identify mutations and Cryo-EM structures of the S protein to model the effects of point mutations (**Fig. 6**). Most of the mutations in the S protein of the B.1.351 variant are localized in the S1 subunit, with only A701V in the S2 subunit. Additionally, three mutations reside in the RBD, among which two of them are not found in the B.1.1.7 variant (K417N, E484K) (**Fig. 6A, 6B**). However, this variant contains D614G and N501Y, which are also seen in the B.1.1.7 variant (**Fig. 5A)**. Furthermore, many of the mutations found in the B.1.351 variant have worldwide frequencies lower than 5%. The exception is D614G, L18F and N501Y (**Fig. 6C, Table 3)**. In comparison to B.1.1.7 and P.1 variants, the B.1.351 variant has not reached a frequency higher than 2% as of April 2021 (**Fig. 4**). By using the mutagenesis tool of PyMOL, we modeled the S protein in complex with hACE2, and with C103 and C121 Nabs, which are human recombinant class I & II neutralizing antibodies, respectively (33). Our *in silico* mutagenesis modelling predicts that B.1.352 mutations in the RBD favor a loss of interactions with C102 and C121 Nabs. Diminished interactions between RBD and C102 are predicted when the K417 is mutated to Asn producing Nabs escape capabilities (**Fig. 6D, 8A).** Diminished interactions with RBD are also predicted with C121 when the E484K mutation is present (**Fig. 6E, 8B)**. As previously mentioned, N501Y is also found in B.1.351 and our modeling predicts that it will have similar effects as those observed with the B.1.1.7 variant (**Fig. 6F**). **Figure 6G** illustrates the position of the nucleotide substitutions of the B.1.351 variant.

The emergence of the P.1 variant in Brazil. Similar to the B.1.351 variant, the P.1 variant harbours the N501Y and E484K mutations, but position 417 of the S protein displays a threonine (T) instead of a lysine (K) residue (23) (**Fig. 7**). Similar to the UK and South African variants, we present in **Figure 7C** mutations in the S protein that are characteristic of the P.1 variant and their frequencies from December 2019 to April 30th 2021. The P.1 variant harbours amino acid substitutions L18F, T20N, P26S, D138Y, and R190S in the NTD of the S protein. H655Y and T1027I, V1176F are in the subdomain 2 (SD2) of S1 and in the S2

subunit, respectively (**Fig. 7A, 7B, Table 4).** The V1176F mutation is not shown because the structure is unresolved in this region. Overall, P.1-specific mutations have currently worldwide frequencies less than 5% (**Fig. 7C, Table 4)**. D614G, L18F and N501Y are not specific to P1. Similar to B.1.351, the P.1 variant has a low frequency representing less than 5% of global variants as of April, 2021 (**Fig. 4**). Here, we also modeled P.1 mutations to investigate interaction alterations with known recombinant neutralizing antibodies (33). The K417T mutation reduces interactions with neighboring residues in the C102 Nab and therefore the model predicts, as with K417N in B.1.1.7, an increased ability to escape neutralization (**Fig. 7D**). Also, the P.1 variant has E484K and N501Y mutations in the RBD. Modelling predicts they will have the same effect reported for the B.1.1.7 and B.1.351 variants (**Fig. 7E, 7F)**. In **Figure 7G**, we indicate the positions of synonymous, non-synonymous, and deletions in the SARS-CoV-2 P.1 genome.

DISCUSSION

The emergence of new genetic variants that are more transmissible, virulent and resistant to antibody neutralization have highlighted the importance of studying the function of mutations in the viral genome. The number of sequenced viral genomes uploaded to the GISAID database grew rapidly from 131,417 at the end of September, 2020 to 451,913 by January 30th, 2021 (28). GISAID is a formidable tool for tracking the emergence of mutations, identifying the geographic region where it emerged, and tracking its spread around the globe. Given the risk mutations and new variants pose for neutralizing antibody therapy and vaccines for SARS-CoV-2, it is crucial to continuously monitor the susceptibility of these variants to neutralization by humoral and cellular immune responses either induced through natural exposure to the reference strain or induced by vaccination (24,25,33). Recent reports on the efficacy of the various vaccines have shown that these are variable and often diminished against variants (**Tables 5 and 6**). Most available vaccines generally remain near fully efficacious against the B.1.1.7 variant (31,34,35). However, the Oxford-AstraZeneca vaccine has displayed compromised efficacy against the B.1.351 variant with only 10% vaccine efficacy (36). Preliminary data with the Pfizer-BioNTech and Moderna mRNA vaccines also show a reduction in efficacy against B.1.351 (35,37,38). Furthermore, antibodies induced by the Pfizer-BioNTech and Moderna vaccines appear to display a 6.7-fold, and 4.5-fold decrease in neutralization efficacy against the P.1 variant (**Table 6)** (39). The recently approved Johnson & Johnson adenovirus-based vaccine only requires a single dose, in comparison to two for the mRNA vaccines and Oxford-AstraZeneca vaccine, and has an efficacy of 66% against the original Wuhan reference strain, 52.0 to 64.0% against the B.1.351 variant and 66% against the P.1 variant (43). The Novavax vaccine also shows reduced efficacy against the variants with 86% and 51% against the B.1.1.7 and P.1 variants, respectively. Nevertheless, humoral responses are only one component of the adaptive immune response. T cell responses have not

been studied in detail against these variants at this time and still provide robust contribution to overall protection against severe COVID-19 disease.

Studying the effect of individual mutations in a viral protein may not always reflect their true impact on virus features if they appear in combination with other mutations. Epistasis is the combinatory effect of two or more mutations in a genome (50). Epistasis has previously been intensely studied in the surface protein hemagglutinin (HA) of influenza viruses and positive epistasis was identified in several regions of the HA receptor-binding domain (51). In relation to the S protein of SARS-CoV-2, epistatic mutations could, for instance, allow the S protein to adopt a specific conformation when all the mutations are present, thereby producing a unique folding of the protein and enabling new features. A recent study demonstrated the impact of antigenicity and infectivity of D614G SARS-CoV-2 variants with a combination of different mutations occurring in the S protein (19). The study shows that D614G alone only mildly increases infectivity, but in combination with different other mutations in the S protein, together these can either more intensely increase or decrease viral infectivity. Similar findings have been reported regarding sensitivity to Nabs. D614G alone has undetectable effects on Nabs escape. However, the combination of D614G with other mutations in S can enable Nabs escape (19). This data suggests that the continuous emergence of epistatic mutations in SARS-CoV-2 will likely be involved in further altering the properties of the virus, including transmissibility, pathogenicity, stability and Nab resistance.

Our analyses have highlighted that several new fast-spreading mutations had frequency trajectories that eventually plunged or stabilized at low frequencies. Only the D614G in the S protein and the P323L in the RdRp have maintained their presence in the consensus sequence (**Fig. 1 and 2**). Analyses of the GISAID database also reveal which countries upload the most sequences to the database and are therefore carrying out the most testing and sequencing. The global frequency of mutations and variants in the database is therefore biased to represent the genetic landscape of the virus in the countries doing the most testing, sequencing, and data sharing. Emergence of new variants may therefore go undetected until they leave their point of origin and enter countries with high testing and sequencing rates. This delayed notification constitutes a major obstacle in identifying and preventing the spread of nefarious variants that are potentially resistant to current vaccines and neutralizing antibody therapy. Another caveat in analyzing sequences in the GISAID database is that consensus sequences are uploaded, but subsequences and quasispecies are generally not included. Therefore, it is possible that mutations in sub-variants may be missed that could contribute to virus replication, pathogenicity, and spread (52). A global approach to analyzing both transmitted variants and non-transmitted sub-variants and quasispecies could provide a better understanding of the effects of SARS-CoV-2 mutations.

In conclusion, our metadata analysis of emerging mutations has highlighted the natural fluctuations in mutation prevalence. We also illustrate how mutations sometimes need to co-emerge in order to create a favorable outcome for virus propagation. Tracking mutations and the evolution of the SARS-CoV-2 genome is critical for the development and deployment of effective treatments and vaccines. Thus, it is the responsibility of all countries and governing jurisdictions to increase testing and sequencing, and uploading SARS-CoV-2 genomes to open access databases in real-time. This will result in more accurate information to inform policy and decision makers about interventions required to blunt the global transmission of the virus and ensure that vaccines remain effective against all circulating variants.

ACKNOWLEDGEMENTS

The authors wish to thank Dr. Sean Li at Health Canada for helpful comments on our manuscript. M.-A.L. holds a Canada Research Chair in Molecular Virology and Intrinsic Immunity. This study was supported by a COVID-19 Rapid Response grant to M-A Langlois by the Canadian Institute of Health Research (CIHR) and by a grant supplement by the Canadian Immunity Task Force (CITF).

CONFLICTS OF INTERESTS

The authors declare no competing interests.

REFERENCES

1. Zhu N, Zhang D, Wang W, Li X, Yang B, Song J, Zhao X, Huang B, Shi W, Lu R, Niu P, Zhan F, Ma X, Wang D, Xu W, Wu G, Gao GF, Tan W. 2020. A Novel Coronavirus from Patients with Pneumonia in China, 2019. *N Engl J Med* **382**:727–733.

2. Dong E, Du H, Gardner L. 2020. An interactive web-based dashboard to track COVID-19 in real time. *The Lancet Infectious Diseases* **20**:533–534.

3. Wu F, Zhao S, Yu B, Chen Y-M, Wang W, Song Z-G, Hu Y, Tao Z-W, Tian J-H, Pei Y-Y, Yuan M-L, Zhang Y-L, Dai F-H, Liu Y, Wang Q-M, Zheng J-J, Xu L, Holmes EC, Zhang Y-Z. 2020. A new coronavirus associated with human respiratory disease in China. *Nature* **579**:265–269.

4. Kim D, Lee J-Y, Yang J-S, Kim JW, Kim VN, Chang H. 2020. The Architecture of SARS-CoV-2 Transcriptome. *Cell 181*:914-921.e10.

5. Duffy S. 2018. Why are RNA virus mutation rates so damn high? *PLOS Biology* **16**:e3000003.

6. Drake JW. 1993. Rates of spontaneous mutation among RNA viruses. Proc Natl Acad Sci USA 90:4171.

7. Peck KM, Lauring AS. 2018. Complexities of Viral Mutation Rates. J Virol 92:e01031-17.

8. Eckerle LD, Becker MM, Halpin RA, Li K, Venter E, Lu X, Scherbakova S, Graham RL, Baric RS, Stockwell TB, Spiro DJ, Denison MR. 2010. Infidelity of SARS-CoV Nsp14-Exonuclease Mutant Virus Replication Is Revealed by Complete Genome Sequencing. *PLOS Pathogens* 6:e1000896.

9. Minskaia E, Hertzig T, Gorbalenya AE, Campanacci V, Cambillau C, Canard B, Ziebuhr J. 2006. Discovery of an RNA virus 3′→5′ exoribonuclease that is critically involved in coronavirus RNA synthesis. *Proc Natl Acad Sci U S A* 103:5108.

10. Ma Y, Wu L, Shaw N, Gao Y, Wang J, Sun Y, Lou Z, Yan L, Zhang R, Rao Z. 2015. Structural basis and functional analysis of the SARS coronavirus nsp14–nsp10 complex. *Proc Natl Acad Sci USA* 112:9436.

11. Rausch JW, Capoferri AA, Katusiime MG, Patro SC, Kearney MF. 2020. Low genetic diversity may be an Achilles heel of SARS-CoV-2. *Proc Natl Acad Sci USA* 117:24614.

12. Chu H, Chan JF-W, Yuen TT-T, Shuai H, Yuan S, Wang Y, Hu B, Yip CC-Y, Tsang JO-L, Huang X, Chai Y, Yang D, Hou Y, Chik KK-H, Zhang X, Fung AY-F, Tsoi H-W, Cai J-P, Chan W-M, Ip JD, Chu AW-H, Zhou J, Lung DC, Kok K-H, To KK-W, Tsang OT-Y, Chan K-H, Yuen K-Y. 2020. Comparative tropism, replication kinetics, and cell damage profiling of SARS-CoV-2 and SARS-CoV with implications for clinical manifestations, transmissibility, and laboratory studies of COVID-19: an observational study. *The Lancet Microbe* 1:e14–e23.

13. Shi J, Wen Z, Zhong G, Yang H, Wang C, Huang B, Liu R, He X, Shuai L, Sun Z, Zhao Y, Liu P, Liang L, Cui P, Wang J, Zhang X, Guan Y, Tan W, Wu G, Chen H, Bu Z. 2020. Susceptibility of

ferrets, cats, dogs, and other domesticated animals to SARS–coronavirus 2. *Science* 368:1016.

14. Li X, Giorgi EE, Marichannegowda MH, Foley B, Xiao C, Kong X-P, Chen Y, Gnanakaran S, Korber B, Gao F. 2020. Emergence of SARS-CoV-2 through recombination and strong purifying selection. *Sci Adv* 6:eabb9153.

15. Walls AC, Park Y-J, Tortorici MA, Wall A, McGuire AT, Veesler D. 2020. Structure, Function, and Antigenicity of the SARS-CoV-2 Spike Glycoprotein. *Cell* 181:281-292.e6.

16. Plante JA, Liu Y, Liu J, Xia H, Johnson BA, Lokugamage KG, Zhang X, Muruato AE, Zou J, Fontes-Garfias CR, Mirchandani D, Scharton D, Bilello JP, Ku Z, An Z, Kalveram B, Freiberg AN, Menachery VD, Xie X, Plante KS, Weaver SC, Shi P-Y. 2020. Spike mutation D614G alters SARS-CoV-2 fitness. *Nature* https://doi.org/10.1038/s41586-020-2895-3.

17. Zhang L, Jackson CB, Mou H, Ojha A, Peng H, Quinlan BD, Rangarajan ES, Pan A, Vanderheiden A, Suthar MS, Li W, Izard T, Rader C, Farzan M, Choe H. 2020. SARS-CoV-2 spike-protein D614G mutation increases virion spike density and infectivity. *Nature Communications* 11:6013.

18. Korber B, Fischer WM, Gnanakaran S, Yoon H, Theiler J, Abfalterer W, Hengartner N, Giorgi EE, Bhattacharya T, Foley B, Hastie KM, Parker MD, Partridge DG, Evans CM, Freeman TM, de Silva TI, Angyal A, Brown RL, Carrilero L, Green LR, Groves DC, Johnson KJ, Keeley AJ, Lindsey BB, Parsons PJ, Raza M, Rowland-Jones S, Smith N, Tucker RM, Wang D, Wyles MD, McDanal C, Perez LG, Tang H, Moon-Walker A, Whelan SP, LaBranche CC, Saphire EO, Montefiori DC. 2020. Tracking Changes in SARS-CoV-2 Spike: Evidence that D614G Increases Infectivity of the COVID-19 Virus. *Cell* 182:812-827.e19.

19. Li Q, Wu J, Nie J, Zhang L, Hao H, Liu S, Zhao C, Zhang Q, Liu H, Nie L, Qin H, Wang M, Lu Q, Li X, Sun Q, Liu J, Zhang L, Li X, Huang W, Wang Y. 2020. The Impact of Mutations in SARS-CoV-2 Spike on Viral Infectivity and Antigenicity. *Cell*, 2020/07/17 ed. 182:1284-1294.e9.

20. Rambaut A, Loman N, Pybus O, Barclay W, Barrett J, Carabelli A, Connor T, Peacock T, Robertson D, Volz E, on behalf of CoG-UK. 2020. Preliminary genomic characterisation of an emergent SARS-CoV-2 lineage in the UK defined by a novel set of spike mutations. https://virological.org/t/preliminary-genomic-characterisation-of-an-emergent-sars-cov-2-lineage-in-the-uk-defined-by-a-novel-set-of-spike-mutations/563

21. O'Toole, A, Hill V, et al. (2021) Tracking the international spread of SARS-CoV-2 lineage B.1.1.7 and B.1.351/501Y-V2. https://virological.org/t/tracking-the-international-spread-of-sars-cov-2-lineages-b-1-1-7-and-b-1-351-501y-v2/592

22. Tegally H, Wilkinson E, Giovanetti M, Iranzadeh A, Fonseca V, Giandhari J, Doolabh D, Pillay S, San EJ, Msomi N, Mlisana K, von Gottberg A, Walaza S, Allam M, Ismail A, Mohale T, Glass AJ, Engelbrecht S, Van Zyl G, Preiser W, Petruccione F, Sigal A, Hardie D, Marais G, Hsiao N, Korsman S, Davies M-A, Tyers L, Mudau I, York D, Maslo C, Goedhals D, Abrahams S, Laguda-Akingba O, Alisoltani-Dehkordi A, Godzik A, Wibmer CK, Sewell BT, Lourenço J, Alcantara LCJ, Kosakovsky Pond SL, Weaver S, Martin D, Lessells RJ, Bhiman JN, Williamson C, de Oliveira T. 2021. Detection

of a SARS-CoV-2 variant of concern in South Africa. *Nature* 592:438–443.

23. Faria, Nuno R.; et al. (12 January 2021). Genomic characterisation of an emergent SARS-CoV-2 lineage in Manaus: preliminary findings. *Virological.* Retrieved 23 January 2021. https://virological.org/t/genomic-characterisation-of-an-emergent-sars-cov-2-lineage-in-manaus-preliminary-findings/586

24. Wang P, Liu L, Iketani S, Luo Y, Guo Y, Wang M, Yu J, Zhang B, Kwong PD, Graham BS, Mascola JR, Chang JY, Yin MT, Sobieszczyk M, Kyratsous CA, Shapiro L, Sheng Z, Nair MS, Huang Y, Ho DD. 2021. Increased Resistance of SARS-CoV-2 Variants B.1.351 and B.1.1.7 to Antibody Neutralization. *bioRxiv* 2021.01.25.428137.

25. Greaney AJ, Starr TN, Gilchuk P, Zost SJ, Binshtein E, Loes AN, Hilton SK, Huddleston J, Eguia R, Crawford KHD, Dingens AS, Nargi RS, Sutton RE, Suryadevara N, Rothlauf PW, Liu Z, Whelan SPJ, Carnahan RH, Crowe JE Jr, Bloom JD. 2021. Complete Mapping of Mutations to the SARS-CoV-2 Spike Receptor-Binding Domain that Escape Antibody Recognition. *Cell Host & Microbe* 29:44-57.e9.

26. Yi C, Sun X, Ye J, Ding L, Liu M, Yang Z, Lu X, Zhang Y, Ma L, Gu W, Qu A, Xu J, Shi Z, Ling Z, Sun B. 2020. Key residues of the receptor binding motif in the spike protein of SARS-CoV-2 that interact with ACE2 and neutralizing antibodies. *Cellular & Molecular Immunology* 17:621–630.

27. Gu H, Chen Q, Yang G, He L, Fan H, Deng Y-Q, Wang Y, Teng Y, Zhao Z, Cui Y, Li Y, Li X-F, Li J, Zhang N-N, Yang X, Chen S, Guo Y, Zhao G, Wang X, Luo D-Y, Wang H, Yang X, Li Y, Han G, He Y, Zhou X, Geng S, Sheng X, Jiang S, Sun S, Qin C-F, Zhou Y. 2020. Adaptation of SARS-CoV-2 in BALB/c mice for testing vaccine efficacy. *Science* 369:1603.

28. Shu Y, McCauley J. 2017. GISAID: Global initiative on sharing all influenza data - from vision to reality. *Euro Surveill* 22:30494.

29. Benton DJ, Wrobel AG, Xu P, Roustan C, Martin SR, Rosenthal PB, Skehel JJ, Gamblin SJ. 2020. Receptor binding and priming of the spike protein of SARS-CoV-2 for membrane fusion. *Nature* 588:327–330.

30. Starr TN, Greaney AJ, Hilton SK, Ellis D, Crawford KHD, Dingens AS, Navarro MJ, Bowen JE, Tortorici MA, Walls AC, King NP, Veesler D, Bloom JD. 2020. Deep Mutational Scanning of SARS-CoV-2 Receptor Binding Domain Reveals Constraints on Folding and ACE2 Binding. *Cell* 182:1295-1310.e20.

31. Haas EJ, Angulo FJ, McLaughlin JM, Anis E, Singer SR, Khan F, Brooks N, Smaja M, Mircus G, Pan K, Southern J, Swerdlow DL, Jodar L, Levy Y, Alroy-Preis S. Impact and effectiveness of mRNA BNT162b2 vaccine against SARS-CoV-2 infections and COVID-19 cases, hospitalisations, and deaths following a nationwide vaccination campaign in Israel: an observational study using national surveillance data. *The Lancet* https://doi.org/10.1016/S0140-6736(21)00947-8.

32. Pereira F. 2020. Evolutionary dynamics of the SARS-CoV-2 ORF8 accessory gene. *Infect Genet Evol*, 2020/09/02 ed. 85:104525–104525.

33. Barnes CO, Jette CA, Abernathy ME, Dam K-MA, Esswein SR, Gristick HB, Malyutin AG, Sharaf NG, Huey-Tubman KE, Lee YE, Robbiani DF, Nussenzweig MC, West AP, Bjorkman PJ. 2020. SARS-CoV-2 neutralizing antibody structures inform therapeutic strategies. *Nature* 588:682–687.

34. Emary KRW, Golubchik T, Aley PK, Ariani CV, Angus B, Bibi S, Blane B, Bonsall D, Cicconi P, Charlton S, Clutterbuck EA, Collins AM, Cox T, Darton TC, Dold C, Douglas AD, Duncan CJA, Ewer KJ, Flaxman AL, Faust SN, Ferreira DM, Feng S, Finn A, Folegatti PM, Fuskova M, Galiza E, Goodman AL, Green CM, Green CA, Greenland M, Hallis B, Heath PT, Hay J, Hill HC, Jenkin D, Kerridge S, Lazarus R, Libri V, Lillie PJ, Ludden C, Marchevsky NG, Minassian AM, McGregor AC, Mujadidi YF, Phillips DJ, Plested E, Pollock KM, Robinson H, Smith A, Song R, Snape MD, Sutherland RK, Thomson EC, Toshner M, Turner DPJ, Vekemans J, Villafana TL, Williams CJ, Hill AVS, Lambe T, Gilbert SC, Voysey M, Ramasamy MN, Pollard AJ. 2021. Efficacy of ChAdOx1 nCoV-19 (AZD1222) vaccine against SARS-CoV-2 variant of concern 202012/01 (B.1.1.7): an exploratory analysis of a randomised controlled trial. *The Lancet* 397:1351–1362.

35. Wu K, Werner AP, Koch M, Choi A, Narayanan E, Stewart-Jones GBE, Colpitts T, Bennett H, Boyoglu-Barnum S, Shi W, Moliva JI, Sullivan NJ, Graham BS, Carfi A, Corbett KS, Seder RA, Edwards DK. 2021. Serum Neutralizing Activity Elicited by mRNA-1273 Vaccine — *Preliminary Report. N Engl J Med* https://doi.org/10.1056/NEJMc2102179

36. Madhi SA, Baillie V, Cutland CL, Voysey M, Koen AL, Fairlie L, Padayachee SD, Dheda K, Barnabas SL, Bhorat QE, Briner C, Kwatra G, Ahmed K, Aley P, Bhikha S, Bhiman JN, Bhorat AE, du Plessis J, Esmail A, Groenewald M, Horne E, Hwa S-H, Jose A, Lambe T, Laubscher M, Malahleha M, Masenya M, Masilela M, McKenzie S, Molapo K, Moultrie A, Oelofse S, Patel F, Pillay S, Rhead S, Rodel H, Rossouw L, Taoushanis C, Tegally H, Thombrayil A, van Eck S, Wibmer CK, Durham NM, Kelly EJ, Villafana TL, Gilbert S, Pollard AJ, de Oliveira T, Moore PL, Sigal A, Izu A. 2021. Efficacy of the ChAdOx1 nCoV-19 Covid-19 Vaccine against the B.1.351 Variant. *N Engl J Med* https://doi.org/10.1056/NEJMoa2102214.

37. Abu-Raddad LJ, Chemaitelly H, Butt AA. 2021. Effectiveness of the BNT162b2 Covid-19 Vaccine against the B.1.1.7 and B.1.351 Variants. *N Engl J Med* https://doi.org/10.1056/NEJMc2104974.

38. Liu Y, Liu J, Xia H, Zhang X, Fontes-Garfias CR, Swanson KA, Cai H, Sarkar R, Chen W, Cutler M, Cooper D, Weaver SC, Muik A, Sahin U, Jansen KU, Xie X, Dormitzer PR, Shi P-Y. 2021. Neutralizing Activity of BNT162b2-Elicited Serum — *Preliminary Report. N Engl J Med* https://doi.org/10.1056/NEJMc2102017.

39. Garcia-Beltran WF, Lam EC, St. Denis K, Nitido AD, Garcia ZH, Hauser BM, Feldman J, Pavlovic MN, Gregory DJ, Poznansky MC, Sigal A, Schmidt AG, Iafrate AJ, Naranbhai V, Balazs AB. 2021. Multiple SARS-CoV-2 variants escape neutralization by vaccine-induced humoral immunity. *Cell* https://doi.org/10.1016/j.cell.2021.03.013.

40. Polack FP, Thomas SJ, Kitchin N, Absalon J, Gurtman A, Lockhart S, Perez JL, Pérez Marc G, Moreira ED, Zerbini C, Bailey R, Swanson KA, Roychoudhury S, Koury K, Li P, Kalina WV, Cooper D, Frenck RW, Hammitt LL, Türeci Ö, Nell H, Schaefer A, Ünal S, Tresnan DB, Mather S, Dormitzer PR, Şahin

U, Jansen KU, Gruber WC. 2020. Safety and Efficacy of the BNT162b2 mRNA Covid-19 Vaccine. *N Engl J Med* 383:2603–2615.

41. Baden LR, El Sahly HM, Essink B, Kotloff K, Frey S, Novak R, Diemert D, Spector SA, Rouphael N, Creech CB, McGettigan J, Khetan S, Segall N, Solis J, Brosz A, Fierro C, Schwartz H, Neuzil K, Corey L, Gilbert P, Janes H, Follmann D, Marovich M, Mascola J, Polakowski L, Ledgerwood J, Graham BS, Bennett H, Pajon R, Knightly C, Leav B, Deng W, Zhou H, Han S, Ivarsson M, Miller J, Zaks T. 2020. Efficacy and Safety of the mRNA-1273 SARS-CoV-2 Vaccine. *N Engl J Med* 384:403–416.

42. Voysey M, Clemens SAC, Madhi SA, et al. 2021. Safety and efficacy of the ChAdOx1 nCoV-19 vaccine (AZD1222) against SARS-CoV-2: an interim analysis of four randomised controlled trials in Brazil, South Africa, and the UK. *The Lancet* 397:99–111.

43. Sadoff J, Gray G, Vandebosch A, Cárdenas V, Shukarev G, Grinsztejn B, Goepfert PA, Truyers C, Fennema H, Spiessens B, Offergeld K, Scheper G, Taylor KL, Robb ML, Treanor J, Barouch DH, Stoddard J, Ryser MF, Marovich MA, Neuzil KM, Corey L, Cauwenberghs N, Tanner T, Hardt K, Ruiz-Guiñazú J, Le Gars M, Schuitemaker H, Van Hoof J, Struyf F, Douoguih M. 2021. Safety and Efficacy of Single-Dose Ad26.COV2.S Vaccine against Covid-19. *N Engl J Med* https://doi.org/10.1056/NEJMoa2101544.

44. Shinde V, Bhikha S, Hoosain Z, Archary M, Bhorat Q, Fairlie L, Lalloo U, Masilela MSL, Moodley D, Hanley S, Fouche L, Louw C, Tameris M, Singh N, Goga A, Dheda K, Grobbelaar C, Kruger G, Carrim-Ganey N, Baillie V, de Oliveira T, Lombard Koen A, Lombaard JJ, Mngqibisa R, Bhorat AE, Benadé G, Lalloo N, Pitsi A, Vollgraaff P-L, Luabeya A, Esmail A, Petrick FG, Oommen-Jose A, Foulkes S, Ahmed K, Thombrayil A, Fries L, Cloney-Clark S, Zhu M, Bennett C, Albert G, Faust E, Plested JS, Robertson A, Neal S, Cho I, Glenn GM, Dubovsky F, Madhi SA. 2021. Efficacy of NVX-CoV2373 Covid-19 Vaccine against the B.1.351 Variant. *N Engl J Med* https://doi.org/10.1056/NEJMoa2103055.

45. Supasa P, Zhou D, Dejnirattisai W, Liu C, Mentzer AJ, Ginn HM, Zhao Y, Duyvesteyn HME, Nutalai R, Tuekprakhon A, Wang B, Paesen GC, Slon-Campos J, López-Camacho C, Hallis B, Coombes N, Bewley KR, Charlton S, Walter TS, Barnes E, Dunachie SJ, Skelly D, Lumley SF, Baker N, Shaik I, Humphries HE, Godwin K, Gent N, Sienkiewicz A, Dold C, Levin R, Dong T, Pollard AJ, Knight JC, Klenerman P, Crook D, Lambe T, Clutterbuck E, Bibi S, Flaxman A, Bittaye M, Belij-Rammerstorfer S, Gilbert S, Hall DR, Williams MA, Paterson NG, James W, Carroll MW, Fry EE, Mongkolsapaya J, Ren J, Stuart DI, Screaton GR. 2021. Reduced neutralization of SARS-CoV-2 B.1.1.7 variant by convalescent and vaccine sera. *Cell* 184:2201-2211.e7.

46. Zhou D, Dejnirattisai W, Supasa P, Liu C, Mentzer AJ, Ginn HM, Zhao Y, Duyvesteyn HME, Tuekprakhon A, Nutalai R, Wang B, Paesen GC, Lopez-Camacho C, Slon-Campos J, Hallis B, Coombes N, Bewley K, Charlton S, Walter TS, Skelly D, Lumley SF, Dold C, Levin R, Dong T, Pollard AJ, Knight JC, Crook D, Lambe T, Clutterbuck E, Bibi S, Flaxman A, Bittaye M, Belij-Rammerstorfer S, Gilbert S, James W, Carroll MW, Klenerman P, Barnes E, Dunachie SJ, Fry EE, Mongkolsapaya J, Ren J, Stuart DI, Screaton GR. 2021. Evidence of escape of SARS-CoV-2 variant B.1.351 from natural and vaccine-induced sera. *Cell* 184:2348-2361.e6.

47. Dejnirattisai W, Zhou D, Supasa P, Liu C, Mentzer AJ, Ginn HM, Zhao Y, Duyvesteyn HME, Tuekprakhon A, Nutalai R, Wang B, Paesen GC, López-Camacho C, Slon-Campos J, Walter TS, Skelly D, Clemens SAC, Naveca FG, Nascimento V, Nascimento F, da Costa CF, Resende PC, Pauvolid-Correa A, Siqueira MM, Dold C, Levin R, Dong T, Pollard AJ, Knight JC, Crook D, Lambe T, Clutterbuck E, Bibi S, Flaxman A, Bittaye M, Belij-Rammerstorfer S, Gilbert S, Carroll MW, Klenerman P, Barnes E, Dunachie SJ, Paterson NG, Williams MA, Hall DR, Hulswit RJG, Bowden TA, Fry EE, Mongkolsapaya J, Ren J, Stuart DI, Screaton GR. 2021. Antibody evasion by the Brazilian P.1 strain of SARS-CoV-2. *bioRxiv* 2021.03.12.435194.

48. Shen X, Tang H, Pajon R, Smith G, Glenn GM, Shi W, Korber B, Montefiori DC. 2021. Neutralization of SARS-CoV-2 Variants B.1.429 and B.1.351. *N Engl J Med* https://doi.org/10.1056/NEJMc2103740.

49. Shen X, Tang H, McDanal C, Wagh K, Fischer W, Theiler J, Yoon H, Li D, Haynes BF, Sanders KO, Gnanakaran S, Hengartner N, Pajon R, Smith G, Glenn GM, Korber B, Montefiori DC. 2021. SARS-CoV-2 variant B.1.1.7 is susceptible to neutralizing antibodies elicited by ancestral spike vaccines. Cell Host & Microbe 29:529-539.e3.

50. Phillips PC. 2008. Epistasis — the essential role of gene interactions in the structure and evolution of genetic systems. *Nature Reviews Genetics* 9:855–867.

51. Wu NC, Xie J, Zheng T, Nycholat CM, Grande G, Paulson JC, Lerner RA, Wilson IA. 2017. Diversity of Functionally Permissive Sequences in the Receptor-Binding Site of Influenza Hemagglutinin. *Cell Host & Microbe* 21:742-753.e8.

52. Rocheleau L, Laroche G, Fu K, Stewart CM, Mohamud AO, Côté M, Giguère PM, Langlois M-A, Pelchat M. 2021. Identification of a High-frequency Intra-host SARS-CoV-2 spike Variant with Enhanced Cytopathic and Fusogenic Effect. *bioRxiv* 2020.12.03.409714.

53. COVID-19 GENOMIC UK CONSORTIUM. 2021. COG-UK report on SARS-CoV-2 Spike mutations of interest in the UK. https://www.cogconsortium.uk/wp-content/uploads/2021/01/Report-2_COG-UK_SARS-CoV-2-Mutations.pdf

54. Zahradník J, Marciano S, Shemesh M, Zoler E, Chiaravalli J, Meyer B, Rudich Y, Dym O, Elad N, Schreiber G. 2021. SARS-CoV-2 RBD *in vitro* evolution follows contagious mutation spread, yet generates an able infection inhibitor. *bioRxiv* 2021.01.06.425392.

55. Kannan SR, Spratt AN, Quinn TP, Heng X, Lorson CL, Sönnerborg A, Byrareddy SN, Singh K. 2020. Infectivity of SARS-CoV-2: there Is Something More than D614G? *J Neuroimmune Pharmacol*, 2020/09/15 ed. 15:574–577.

56. Ugurel OM, Mutlu O, Sariyer E, Kocer S, Ugurel E, Inci TG, Ata O, Turgut-Balik D. 2020. Evaluation of the potency of FDA-approved drugs on wild type and mutant SARS-CoV-2 helicase (Nsp13). *Int J Biol Macromol*, 2020/09/24 ed. 163:1687–1696.

57. Wu S, Tian C, Liu P, Guo D, Zheng W, Huang X, Zhang Y, Liu L. 2020. Effects of SARS-CoV-2 mutations on protein structures and intraviral protein–protein interactions. *Journal of Medical*

Virology. 2021;93:2132–2140.

58. Weisblum Y, Schmidt F, Zhang F, DaSilva J, Poston D, Lorenzi JC, Muecksch F, Rutkowska M, Hoffmann H-H, Michailidis E, Gaebler C, Agudelo M, Cho A, Wang Z, Gazumyan A, Cipolla M, Luchsinger L, Hillyer CD, Caskey M, Robbiani DF, Rice CM, Nussenzweig MC, Hatziioannou T, Bieniasz PD. 2020. Escape from neutralizing antibodies by SARS-CoV-2 spike protein variants. *eLife* 9:e61312.

TABLES

Table 1: Non-synonymous mutations in SARS-CoV-2 genes with a worldwide frequency ≥0.01%.

Protein (Gene)	Genome Nucleotide Mutation	Codon	AA Mutation	Frequency (%)*	Effect
S	A23403G	G**A**T to G**G**T	D614G	99.70	Moderate increase in Transmissibility[53]
	C22227T	G**C**T to G**T**T	A222V	42.79	No effect[53]
	C21615T	**C**TT to **T**TT	L18F	19.86	N/A
	G22992A	A**G**C to A**A**C	S477N	5.36	Spike-hACE2 complex stability and Nab interference[54]
	C22879A	AA**C** to AA**A**	N439K	4.09	Antibody escape ability[19,53]
	C21575T	**C**TT to **T**TT	L5F	1.44	N/A
	C21855T	T**C**T to T**T**T	S98F	2.74	N/A
	G22346T	**G**CT to **T**CT	A262S	1.64	N/A
	A23063T	**A**AT to **T**AT	N501Y	80.16	Increase affinity for hACE2[53]
	C23709T	A**C**A to A**T**A	T716I	75.37	N/A
	C23271A	G**C**T to G**A**T	A570D	76.30	N/A
	G24914C	**G**CA to **C**AC	D1118H	74.82	N/A
	C23709A	C**C**T to C**A**T	P681H	79.18	N/A
	T24506G	**T**CA to **G**CA	S982A	74.61	N/A
	21765-21770del	**N/A**	ΔH69/ΔV70	75.13	Antibody escape[53]
	21991-21993del	**N/A**	ΔY144	76.91	Decrease infectivity, antibody escape[19]
NSP1 (ORF1ab)	C335T	**C**GC to **T**GC	R24C	0.38	N/A
NSP2 (ORF1ab)	G1210T	AT**G** to AT**T**	M135I	0.01	N/A
	C1059T	A**C**C to A**T**C	T85I	13.95	N/A
	T1947C	G**T**T to G**C**T	V381A	1.08	N/A
	C2453T	**C**TC to **T**TC	L550F	5.93	N/A
NSP3 (ORF1ab)	C7926T	G**C**A to G**T**A	A1736V	0.12	N/A
	T7767C	A**T**C to A**C**C	I1683T	0.19	N/A
	C5622T	C**C**T to C**T**T	P968L	0.09	N/A
	G8371T	CA**G** to CA**T**	Q1884H	0.05	N/A
	C4002T	A**C**T to A**T**T	T428I	0.44	N/A
	C5388A	G**C**T to G**A**T	A890D	76.25	N/A
	G8083A	AT**G** to AT**A**	M1788I	0.68	N/A
	C3602T	**C**AC to **T**AC	H295Y	0.30	N/A
NSP4 (ORF1ab)	C9246T	G**C**T to G**T**T	A231V	0.12	N/A
	G9526T	AT**G** to AT**T**	M324I	0.14	N/A
NSP5 (ORF1ab)	A10323G	A**A**G to A**G**G	K90R	3.07	N/A
	G10097A	**G**GT to **A**GT	G15S	0.35	N/A
	C10319T	**C**TT to **T**TT	L89F	1.44	N/A
NSP6 (ORF1ab)	C11109T	G**C**T to G**T**T	A46V	0.15	N/A
	C11396T	**C**TT to **T**TT	L142F	0.02	N/A
	G11083T	TTG to TT**T**	L37F	1.26	N/A
	C11195T	**C**TT to **T**TT	L75F	0.13	N/A
	G11230T	AT**G** to AT**T**	M86I	0.03	N/A
	G11801A	**G**GT to **A**GT	G277S	0.07	N/A
	G11132T	**G**CT to **T**CT	A54S	0.02	N/A
	11288-11296 del	N/A	ΔS106/ΔG3676/ΔF3677	87.61	N/A

NSP7	G12067T	AT**G** to AT**T**	M75I	0.15	N/A
(ORF1ab)	C11916T	T**C**A to T**T**A	S25L	0.10	N/A
NSP9	G12988T	AT**G** to AT**T**	M101I	0.23	N/A
(ORF1ab)					
NSP12	C14408T	C**C**T to C**T**T	P323L	99.49	Improves processivity by
(ORF1ab)					interaction with NSP8[55]
	G15766T	**G**TG to **T**TG	V776L	0.14	N/A
	G13993T	**G**CT to **T**CT	A185S	0.09	N/A
	G15598A	**G**TC to **A**TC	V720I	0.17	N/A
	G14202T	GA**G** to GA**T**	E254D	0.01	N/A
	C13730T	G**C**T to G**T**T	A97V	0.35	N/A
NSP13	C16289T	G**C**T to G**T**T	A18V	0.03	N/A
(ORF1ab)	G17019T	GA**G** to GA**T**	E261D	0.22	N/A
	C17104T	**C**AT to **T**AT	H290Y	0.23	N/A
	C17747T	C**C**T to C**T**T	P504L	0.07	Increases hydrophobicity of 2A
					domain[56]
	C17639T	T**C**A to T**T**A	S468L	0.02	N/A
	A17615G	A**A**G to A**G**G	K460R	15.82	N/A
	A16889G	A**A**A to A**G**A	K218R	0.08	N/A
	G18028T	**G**CA to **T**CA	A598S	0.26	N/A
NSP14	C18998T	G**C**A to G**T**A	A320V	0.01	N/A
(ORF1ab)	C18568T	**C**TC to **T**TC	L177F	0.22	N/A
	G19542T	AT**G** to AT**T**	M501I	0.21	N/A
	A18424G	**A**AT to **G**AT	N129D	1.37	N/A
NSP15	C19718T	A**C**A to A**T**A	T33I	0.06	N/A
(ORF1ab)					
NSP16	A21137G	A**A**G to A**G**G	K160R	4.69	N/A
(ORF1ab)	A21390G	TT**A** to TT**G**	R216C	1.30	N/A
N	C28932T	G**C**T to G**T**T	A220V	0.38	N/A
	G28580T	**G**AT to **T**AT	D103Y	0.02	N/A
	G28883C	**G**GA to **C**GA	G204R	75.15	Destabilizes N protein[57]
	C28311T	C**C**C to C**T**C	P13L	2.00	N/A
	C28869T	C**C**A to C**T**A	P199L	5.55	N/A
	G28882A	A**G**C to A**A**A	R203K	81.96	Destabilizes N protein[57]
	C28883A	AG**C** to AA**A**	R203K	81.96	Destabilizes N protein[57]
	C28854T	T**C**A to T**T**A	S194L	0.33	Destabilizes N protein[57]
	C28977T	T**C**T to T**T**T	S235F	76.34	N/A
	G28280C	**G**AT to **C**TA	D3L	75.53	N/A
	A28281T	GA**T** to C**T**A	D3L	75.53	N/A
	T28282A	GA**T** to CT**A**	D3L	75.53	N/A
	G28975C	AT**G** to AT**C**	M234I	7.58	N/A
	C28472T	**C**CT to **T**CT	P67S	1.38	N/A
	G29399A	**G**CT to **A**CT	A376T	0.09	N/A
	C29366T	**C**CA to **T**CA	P365S	0.15	N/A
	G29402T	**G**AT to **T**AT	D377Y	1.61	N/A
	C28887T	A**C**T to A**T**T	T205I	7.00	N/A
	C29466T	G**C**A to G**T**A	A398V	0.51	N/A
M	A26530G	GA**T** to G**G**T	D3G	0.01	N/A
	C27046T	A**C**G to A**T**G	T175M	0.02	N/A
NS3	G25907T	G**G**T to G**T**T	G172V	1.41	N/A
(ORF3a)	G25617T	AA**G** to AA**T**	K75N	0.02	N/A

	G25563T	CA**G** to CA**T**	Q57H	14.36	N/A
	C26060T	A**C**T to A**T**T	T223I	0.38	N/A
	G25429T	**G**TA to **T**TA	V13L	0.05	N/A
	G25996T	**G**TA to **T**TA	V202L	0.17	N/A
	A25505G	C**A**A to C**G**A	Q38R	0.04	N/A
	G25906C	**G**GT to **C**GT	G172R	5.31	N/A
NS7b	A27866T	C**A**T to C**T**A	H37L	0.01	N/A
(ORF7b)	AT27867A	CA**T** to CT**A**	H37L	0.01	N/A
	C27769T	T**C**A to T**T**A	S5L	0.07	N/A
NS8	C28087T	G**C**T to G**T**T	A65V	0.77	N/A
(ORF8)	T28144C	T**T**A to T**C**A	L84S	0.14	N/A
	C27964T	T**C**A to T**T**A	S24L	1.38	N/A
	G28077T	**G**TG to **T**TG	V62L	0.24	N/A
	C27972T	**C**AA to **T**AA	Q27stop	76.05	Inactivates NS8[32]
	G28048T	A**G**A to A**T**A	R52I	76.00	N/A

* Mutation frequency as of April 30th, 2021.

Table 2: Synonymous, non-synonymous and deletion mutations in the B.1.1.7 variant

Variant	Protein (Gene)	Genome Nucleotide Mutation	S or NS	AA mutation[20]	Domain	Frequency* (%)	Effect
B.1.1.7	*NSP2 (ORF1ab)*	C913T	S			N/A	N/A
	NSP3 (ORF1ab)	C3267T	NS	T183I		76.14	N/A
		C5388A	NS	A890D		76.24	N/A
		C5986T	S			N/A	N/A
		T6954C	NS	I1412T		75.21	N/A
	NSP6 (ORF1ab)	11288-11296del	NS	ΔS106/ ΔG107/ΔF108		87.61	N/A
	NSP12 (ORF1ab)	C14676T	S			N/A	N/A
		C15279T	S			N/A	N/A
	NSP13 (ORF1ab)	C16176T	S			N/A	N/A
	S	21765-21770del	NS	ΔH69/ΔV70	NTD	75.13	Antibody escape[53]
		21991-21993del	NS	ΔY144	NTD	76.91	Decreases infectivity, Antibody escape[19]
		A23063T	NS	N501Y	RBD	80.16	Increases affinity for hACE2[51]
		C23271A	NS	A570D	SD1	76.30	
		A23403G	NS	D614G	SD2	99.29	Moderate increase in transmissibility[19, 51]
		C23709A	NS	P681H	SD2	79.18	N/A
		C23709T	NS	T716I		75.37	N/A
		T24506G	NS	S982A	HR1	74.61	N/A
		G24914C	NS	D1118H		74.82	N/A
	NS8 (ORF8)	C27972T	NS	Q27stop		76.05	Inactivation of NS8[32]
		G28048T	NS	R52I		76.00	N/A
		A28111G	NS	Y73C		76.07	N/A
	M	T26801C	S			N/A	N/A
	N	G28280C	NS	D3L		75.53	N/A
		A28281T	NS	D3L		75.53	N/A
		T28282A	NS	D3L		75.53	N/A
		C28977T	NS	S235F		76.34	N/A

* Mutation frequency as of April 30th, 2021.

Table 3: Synonymous, non-synonymous mutations and deletions in the B.1.351 variant

Variant	Protein (Gene)	Genome Nucleotide Mutation[22]	S or NS	A.A mutation	Domain	Frequency * (%)	Effect
B.1.351	*5'-UTR*	G174T	**S**			N/A	N/A
	NSP2 (ORF1ab)	C1059T	NS	T85I		13.95	N/A
		A2692T	S			N/A	N/A
	NSP3 (ORF1ab)	G5230T	NS	K837N		1.41	N/A
	NSP5 (ORF1ab)	A10323G	NS	K90R		3.07	N/A
	NSP12 (ORF1ab)	C14925T	S			N/A	N/A
	S	C21614T	NS	L18F	NTD	4.11	N/A
		A21801C	NS	D80A	NTD	0.50	N/A
		A22206G	NS	D215G	NTD	0.51	N/A
		22286-22294del	NS	ΔL242/ΔA243/ΔL244	NTD	0.51	Antibody escape[58]
		G22299T	NS	R246I	NTD	0.004	Antibody escape[58]
		G22813T	NS	K417N	RBD	0.51	Antibody escape[24]
		G23012A	NS	E484K	RBD	3.51	Antibody escape[33,53]
		A23063T	NS	N501Y	RBD	80.16	Increases affinity for hACE2[51]
		A23403G	NS	D614G	SD2	99.29	Moderate increase in transmissbility[19,53]
		G23664T	NS	A701V	S1/S2 – S2'	2.15	N/A
	NS3 (ORF3a)	G25563T	NS	Q57H		14.36	N/A
		C25904T	NS	S171L		1.77	N/A
	E	C26456T	NS	P71L		1.42	N/A
	M	C26645T	S				N/A
	NS7a (ORF7a)	T27504C	S				N/A
	N	C28887T	NS	T205I		7.00	N/A

* Mutation frequency as of April 30th, 2021.

Table 4: Synonymous, non-synonymous and deletions in the P.1 variant.

Variant	Protein (Gene)	Genome Nucleotide Mutation[23]	S or NS	A.A mutation	Domain	Frequency* (%)	Effect
P.1	*NSP2 (ORF1ab)*	T733C	S			N/A	N/A
		C2749T	S			N/A	N/A
	NSP3 (ORF1ab)	C3828T	NS	S370L		3.09	N/A
		A5648C	NS	K977Q		3.00	N/A
	NSP6 (ORF1ab)	11288-11296del	NS	ΔS106/ ΔG107/ΔF 108		87.61	N/A
	NSP9 (ORF1ab)	C12778T	S			N/A	N/A
	NSP12 (ORF1ab)	C13860T	S			N/A	N/A
	NSP13 (ORF1ab)	G17259T	NS	E341D		2.97	N/A
	S	C21614T	NS	L18F	NTD	4.11	N/A
		C21621A	NS	T20N	NTD	2.77	N/A
		C21638T	NS	P26S	NTD	3.01	N/A
		G21974T	NS	D138Y	NTD	2.95	N/A
		G22132T	NS	R190S	NTD	2.71	N/A
		A22812C	NS	K417T	RBD	2.88	Antibody escape[39]
		G23012A	NS	E484K	RBD	3.51	Antibody escape[33,53]
		A23063T	NS	N501Y	RBD	80.16	Increase affinity for hACE2[53]
		A23403G	NS	D614G	SD2	99.29	Moderate increase in transmissibility [19,53]
		C23525T	NS	H655Y	SD2	3.16	N/A
		C24642T	NS	T1027I	S2	2.79	N/A
		G25088T	NS	V1176F	S2	2.79	N/A
	NS8 (ORF8)	G28167A	NS	E92K		2.96	N/A
		Ins28269-28273	S			N/A	N/A
	N	C28512G	NS	P80R		2.94	N/A

* Mutation frequency as of April 30th, 2021.

Table 5: Efficacy of Vaccines Against SARS-CoV-2 Variants

Vaccine	hCoV-19/Wuhan/WIV-4/2019	B.1.1.7	B.1.351	P.1
Pfizer-BioNTech	95.0%[40]	95.3%[31,37]	75.0%[37]	N/A
Moderna	94.1%[41]	N/A	N/A	N/A
Oxford-AstraZeneca	70.4%[42]	70.4%[34]	10%[36]	N/A
Johnson & Johnson	66%[43]	N/A	52.0% and 64.0% (14 and 28 days)[43]	66%[43]
Novavax	96%[44]	86%[44]	51%[44]	

Table 6: Resistance of SARS-CoV-2 Variants to Vaccine-Induced Antibody Neutralization

Vaccine	Fold Reduction in Neutralization		
	B.1.1.7	B.1.351	P.1
Pfizer-BioNTech	[a]2.1 [39]	[a](34.5-42.4) [39]	[a]6.7 [39]
Moderna	[a]2.3 [39]	[a](19.2-27.7)[39]	[a]4.5 [39]
Oxford-AstraZeneca	[b]2.5 [45]	[b]9.0 [46]	[b]2.6 [47]
Johnson & Johnson	N/A	N/A	N/A
Novavax	[a](0.85 to 20) [48]	[a]13.1 [49]	N/A

[a]Pseudotyped virus neutralization assay.

[b]Live virus neutralization assay.

FIGURE LEGENDS

Figure 1: Variations in mutations and mutation frequencies in SARS-CoV-2 genes. The occurrence and frequency of mutations in various SARS-CoV-2 genes are presented for the period between December 2019 to January 1st, 2021. Plotted are mutations that reached at least a 1% worldwide frequency. SARS-CoV-2 genes are represented with the function of the genes in parentheses. A) Genes with <10 mutations. B) Genes with >10 mutations. Graphs were generated using RStudio. *overlapping curves

Figure 2: Geographic location and timeline of dominant mutations in NSP12, S, and N genes. A) Frequency of S protein mutations with corresponding geographic maps. B) Frequency of RdRp mutations with corresponding geographic maps. C) Frequency of Nucleoprotein mutations with corresponding geographic maps. D) Timeline of the appearance of mutations reaching a frequency higher than 50% worldwide between December, 2019 and April, 2021. For the geomaps: a low frequency of reported cases of the mutations is represented in white, while higher frequencies are represented from pink to red, and grey represents no data. All maps were taken from GISAID. Graphs were generated using RStudio and Biorender. *overlapping curves

Figure 3: Structural rendering of the most frequent mutations in the S protein. A) Surface representation of hACE2 (yellow) in complex with S protein trimers illustrated in grey, blue, and magenta. Interactions of high frequency mutations are presented as follows: B) A222V, C) S477N, D) L18F, E) D614G in the open conformation and F) D614G in the closed conformation. Reference sequence residues are illustrated in green, and the mutated amino acid is represented in purple. The red markers illustrate the steric clash when the mutations are inserted into the structure. Graphs were generated using PyMOL.

Figure 4: Worldwide frequency of B.1.1.7, B.1.351, P.1 and D614G variants. Database variants frequency were analyzed from December, 2019 to April 30th, 2021. hCoV-19/Wuhan is the original reference strain and hCoV-19/D614G is the current reference strain containing the D614G mutation in the S protein. B.1.1.7, B.1.353, and P.1 represent the UK, South African, and Brazilian variants. *overlapping curves.

Figure 5: Analysis of mutations in the B.1.1.7 variant. A) Mutation map of the spike protein of B.1.1.7. B) Structural representation of spike with ACE2. B.1.1.7 S protein mutations are presented in in red. NTD (green), RBD (blue), SD1 (purple), SD2 (light blue), and S2 (magenta) are illustrated. The other S protein

monomers are displayed in grey and white. C) Frequency of the mutations in the S protein, B.1.1.7 variant from December, 2019 to April 30th, 2021. D) Interaction of the N501Y (red) mutation in the RBD (blue) of S protein with hACE2 (yellow). The dash lines indicate interactions with adjacent residues. E) Genome of the SARS-CoV-2 B.1.1.7 variant with identified nucleotide substitutions and deletions. Graphs were generated using Biorender, PyMOL, and RStudio. *overlapping curves.

Figure 6: Analysis of mutations in the B.1.351 variant. A) Mutation map of the spike protein of B.1.351. B) Structural representation of spike with ACE2. B.1.352 S protein mutations are presented in orange. NTD (green), RBD (blue), SD1 (purple), SD2 (light blue), and S2 (magenta) are illustrated. The other S protein monomers are illustrated in grey and white. C) Frequency of the mutations in the S protein B.1.351 variant from December, 2019 to April 30th, 2021. Interaction of D) 417N with C102 Nab (green), E) 484K with C121 Nab (light pink), and F) 501Y with hACE2 (yellow). The mutant residues are illustrated in orange, and the dashed lines represent interactions with adjacent residues. G) Genome of the SARS-CoV-2 B.1.351 variant with identified nucleotide substitutions or deletions. Graphs were generated using Biorender, PyMOL, and RStudio. *overlapping curves.

Figure 7: Analysis of mutations in the P.1 variant. A) Mutation map of the spike protein of P.1. B) Structural representation of spike with ACE2. P.1 S protein mutations are presented in black. NTD (green), RBD (blue), SD1 (purple), SD2 (light blue), and S2 (magenta) are illustrated. The other S protein monomers are illustrated in grey and white. C) Frequency of P.1 variant S protein mutations from December 2019 to April 30th 2021. Interaction of D) 417T with C102 Nab (green), E) 484K with C121 Nab (light pink), and F) 501Y with hACE2 (yellow). The mutations are coloured in black and interaction with adjacent residues are demonstrated by dashed lines. G) Genome of the SARS-CoV-2 P.1 variant with identified nucleotides substitution, deletions, and insertions. Figures were generated using Biorender, PyMOL and RStudio. *overlapping curves.

Figure 8: Interactions of K417, E484, and N501 of the S protein with neutralizing antibodies and hACE2. A) Interaction of K417 (blue) with C102 Nab (green) residues. B) Interaction of E484 (blue) with C121 Nab (light pink). C) Interaction of N501 (blue) with hACE2 (yellow) Dashes lines indicate interactions between residues. The graphs were generated using PyMOL.

Figure 1

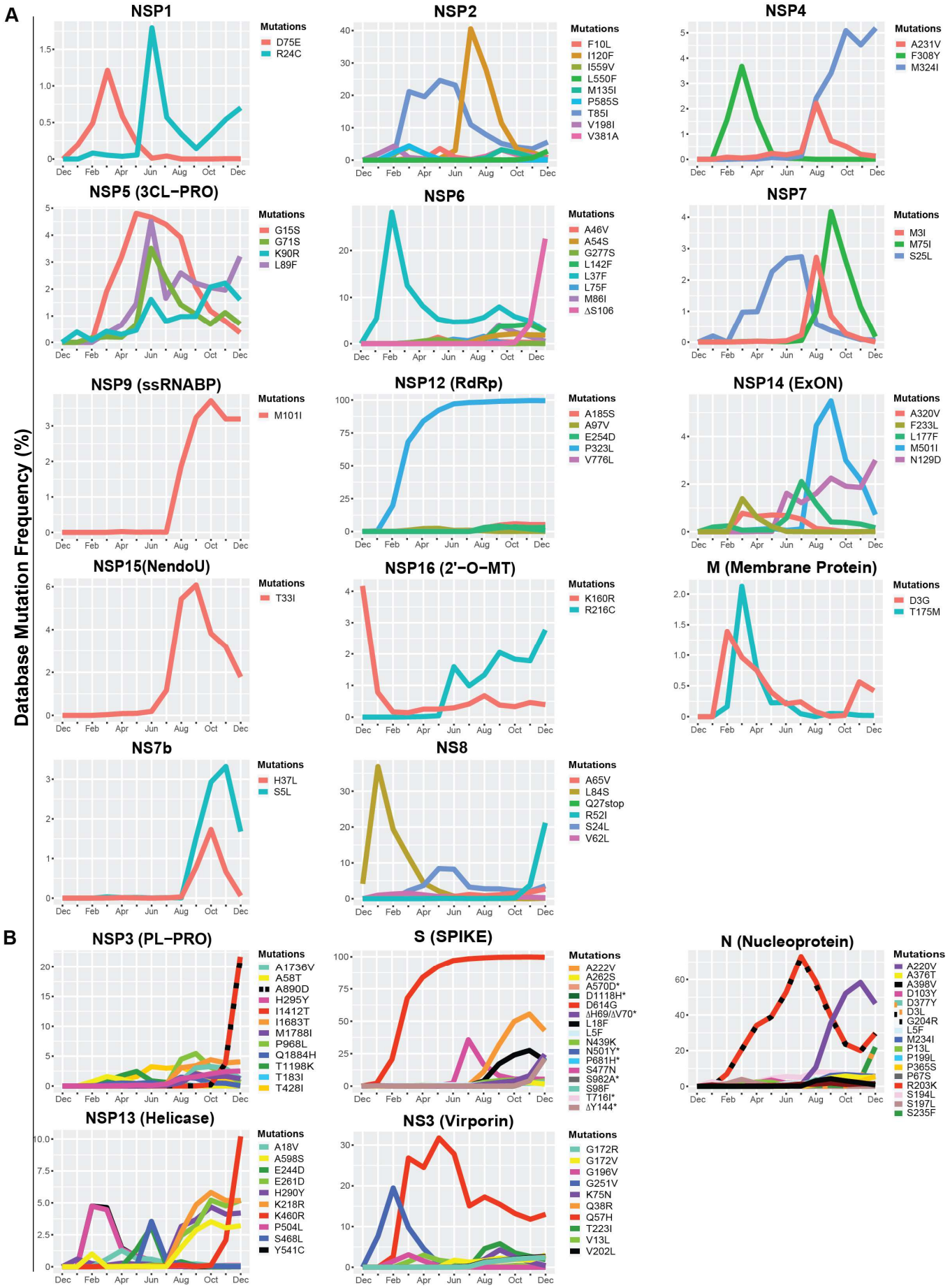
A
B
Database Mutation Frequency (%)
NSP1
Mutations
D75E
R24C
NSP2
Mutations
F10L
I120F
I559V
L550F
M135I
P585S
T85I
V198I
V381A
NSP4
Mutations
A231V
F308Y
M324I
NSP5 (3CL−PRO)
Mutations
G15S
G71S
K90R
L89F
NSP6
Mutations
A46V
A54S
G277S
L142F
L37F
L75F
M86I
ΔS106
NSP7
Mutations
M3I
M75I
S25L
NSP9 (ssRNABP)
Mutations
M101I
NSP12 (RdRp)
Mutations
A185S
A97V
E254D
P323L
V776L
NSP14 (ExON)
Mutations
A320V
F233L
L177F
M501I
N129D
NSP15(NendoU)
Mutations
T33I
NSP16 (2'−O−MT)
Mutations
K160R
R216C
M (Membrane Protein)
Mutations
D3G
T175M
NS7b
Mutations
H37L
S5L
NS8
Mutations
A65V
L84S
Q27stop
R52I
S24L
V62L
NSP3 (PL−PRO)
Mutations
A1736V
A58T
A890D
H295Y
I1412T
I1683T
M1788I
P968L
Q1884H
T1198K
T183I
T428I
S (SPIKE)
Mutations
A222V
A262S
A570D*
D1118H*
D614G
ΔH69/ΔV70*
L18F
L5F
N439K
N501Y*
P681H*
S477N
S982A*
S98F
T716I*
ΔY144*
N (Nucleoprotein)
Mutations
A220V
A376T
A398V
D103Y
D377Y
D3L
G204R
L5F
M234I
P13L
P199L
P365S
P67S
R203K
S194L
S197L
S235F
NSP13 (Helicase)
Mutations
A18V
A598S
E244D
E261D
H290Y
K218R
K460R
P504L
S468L
Y541C
NS3 (Virporin)
Mutations
G172R
G172V
G196V
G251V
K75N
Q38R
Q57H
T223I
V13L
V202L
Dec
Feb
Apr
Jun
Aug
Oct
Dec

Figure 2

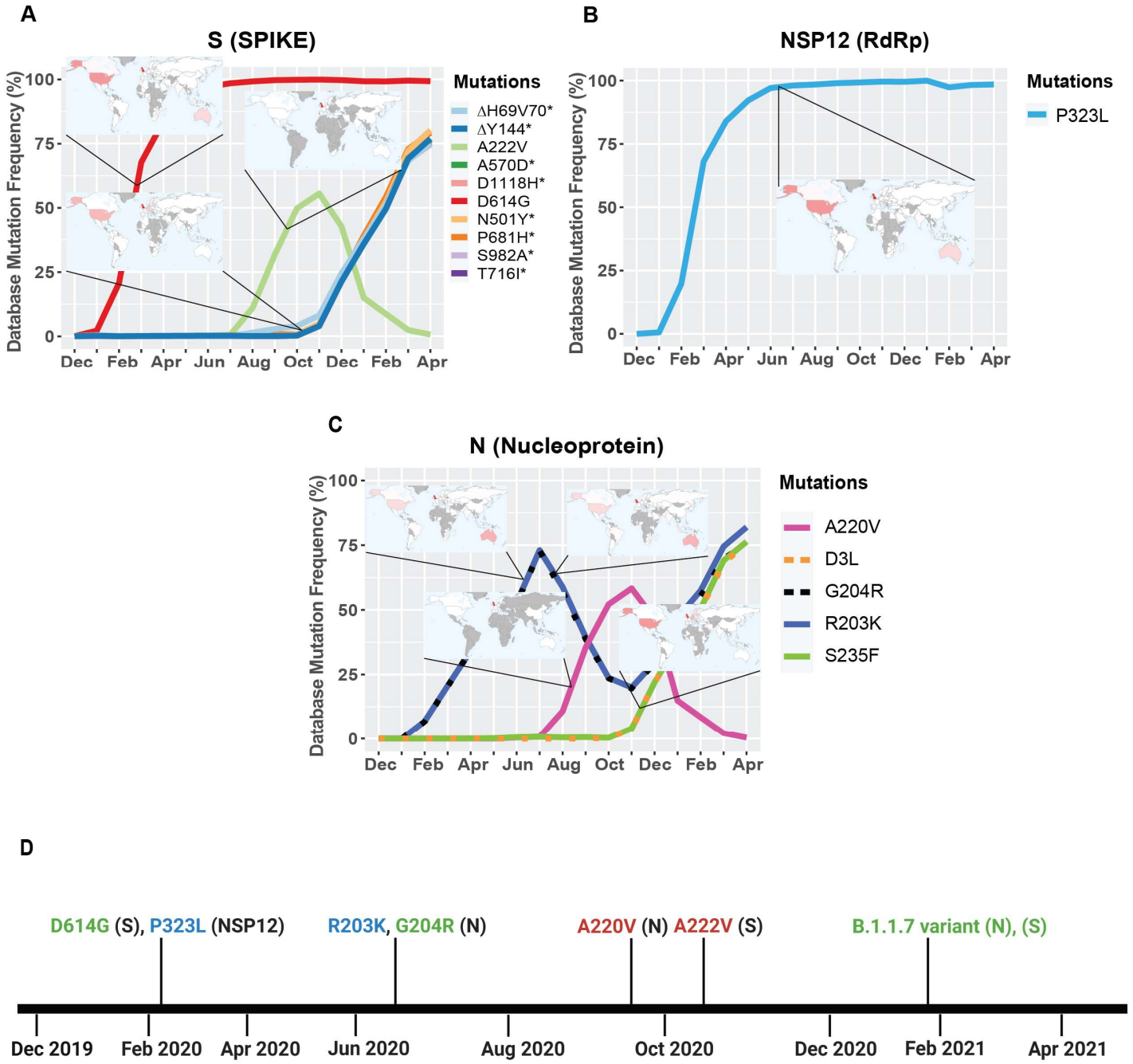
A
S (SPIKE)
Database Mutation Frequency (%)
100
75
50
25
0
Dec Feb Apr Jun Aug Oct Dec Feb Apr
Mutations
ΔH69V70*
ΔY144*
A222V
A570D*
D1118H*
D614G
N501Y*
P681H*
S982A*
T716I*
B
NSP12 (RdRp)
Database Mutation Frequency (%)
100
75
50
25
0
Dec Feb Apr Jun Aug Oct Dec Feb Apr
Mutations
P323L
C
N (Nucleoprotein)
Database Mutation Frequency (%)
100
75
50
25
0
Dec Feb Apr Jun Aug Oct Dec Feb Apr
Mutations
A220V
D3L
G204R
R203K
S235F
D
D614G (S), P323L (NSP12)
R203K, G204R (N)
A220V (N) A222V (S)
B.1.1.7 variant (N), (S)
Dec 2019
Feb 2020
Apr 2020
Jun 2020
Aug 2020
Oct 2020
Dec 2020
Feb 2021
Apr 2021

Figure 3

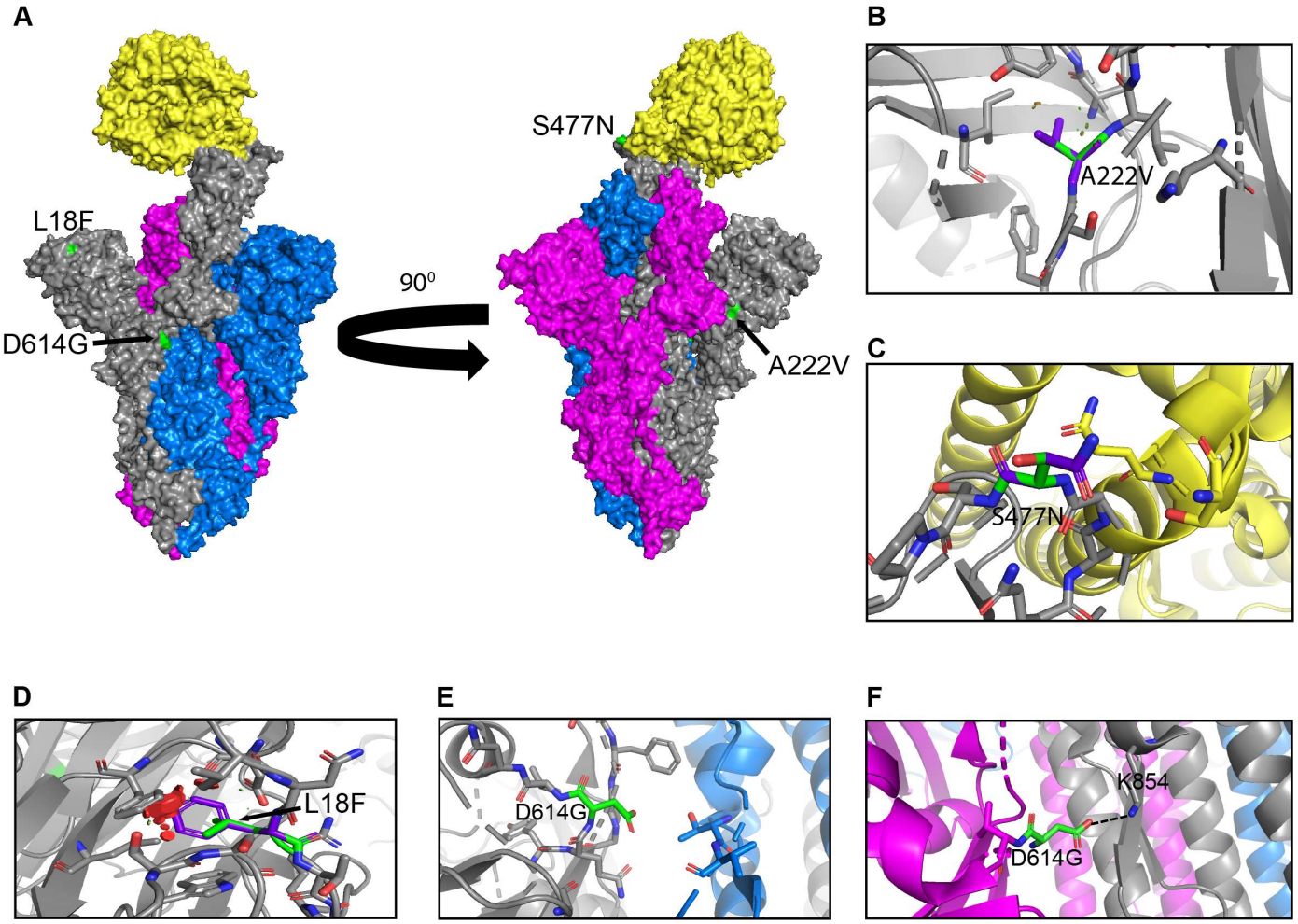
A
L18F
D614G
90⁰
S477N
A222V
B
A222V
C
S477N
D
L18F
E
D614G
F
K854
D614G

Figure 4

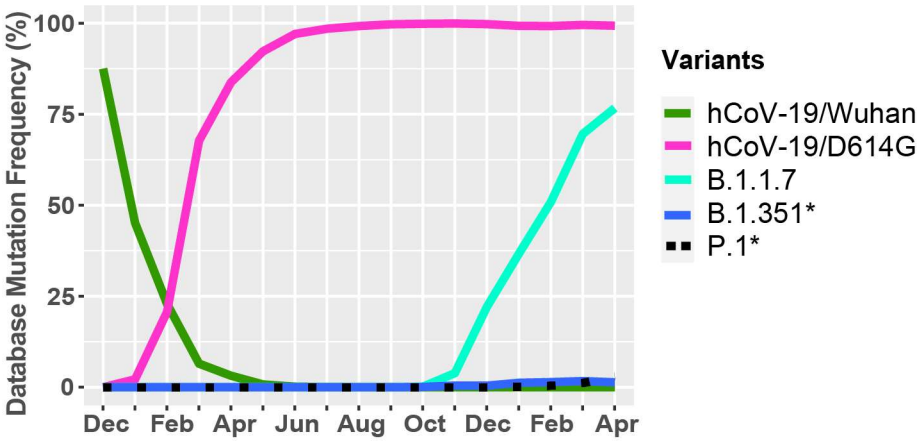
Database Mutation Frequency (%)
100
75
50
25
0
Dec
Feb
Apr
Jun
Aug
Oct
Dec
Feb
Apr
Variants
hCoV-19/Wuhan
hCoV-19/D614G
B.1.1.7
B.1.351*
P.1*

Figure 5

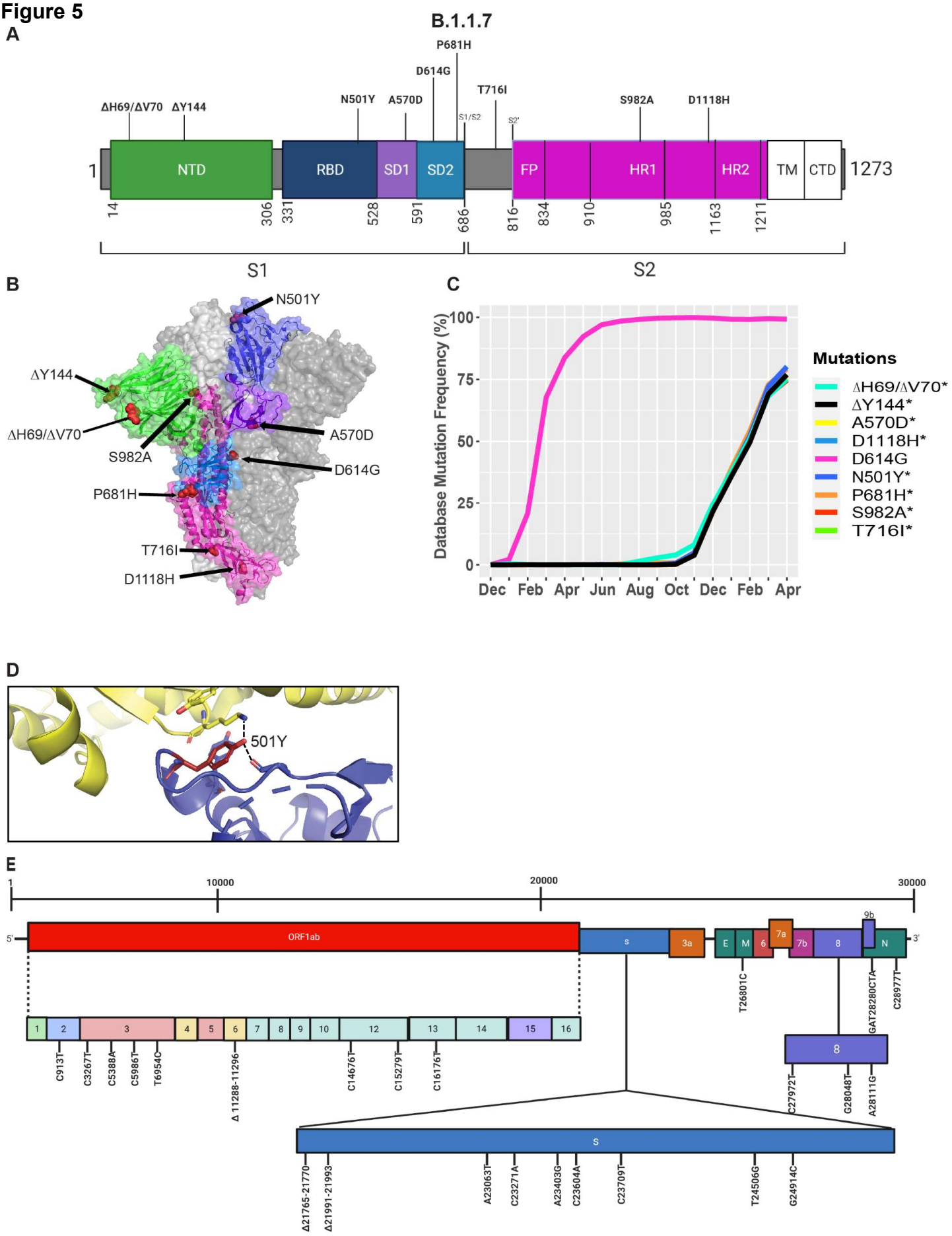
A
B.1.1.7
P681H
D614G
T716I
ΔH69/ΔV70
ΔY144
N501Y
A570D
S982A
D1118H
S1/S2
S2'
1
NTD
RBD
SD1
SD2
FP
HR1
HR2
TM
CTD
1273
14
306
331
528
591
686
816
834
910
985
1163
1211
S1
S2
B
N501Y
ΔY144
ΔH69/ΔV70
S982A
A570D
D614G
P681H
T716I
D1118H
C
Database Mutation Frequency (%)
100
75
50
25
0
Dec
Feb
Apr
Jun
Aug
Oct
Dec
Feb
Apr
Mutations
ΔH69/ΔV70*
ΔY144*
A570D*
D1118H*
D614G
N501Y*
P681H*
S982A*
T716I*
D
501Y
E
1
10000
20000
30000
5'
3'
ORF1ab
s
3a
E
M
6
7a
7b
8
9b
N
T26801C
GAT28280CTA
C28977T
1
2
3
4
5
6
7
8
9
10
12
13
14
15
16
C913T
C3267T
C5388A
C5986T
T6954C
Δ 11288-11296
C14676T
C15279T
C16176T
8
C27972T
G28048T
A28111G
S
Δ21765-21770
Δ21991-21993
A23063T
C23271A
A23403G
C23604A
C23709T
T24506G
G24914C

Figure 6

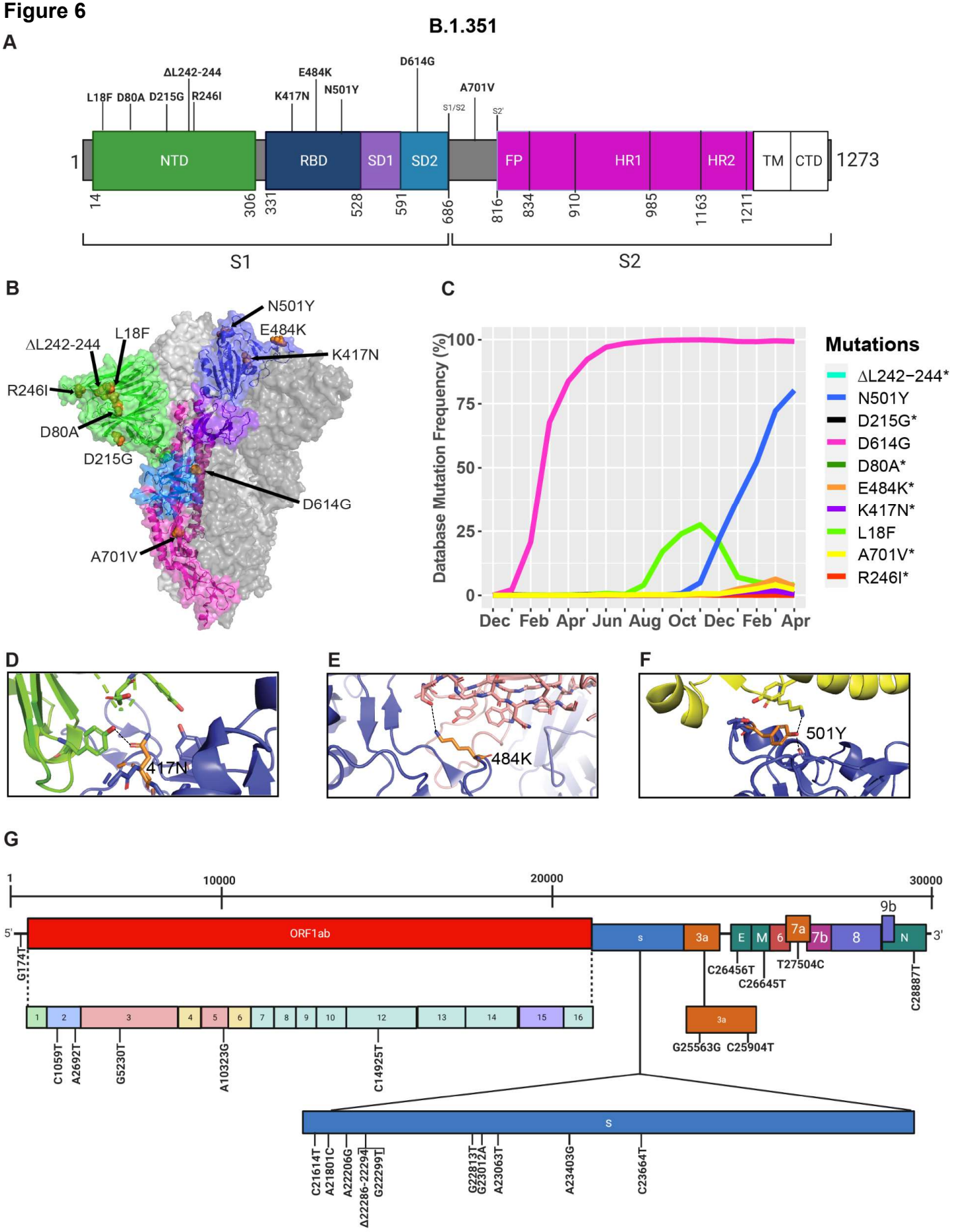
B.1.351
A
ΔL242-244
L18F D80A D215G R246I
E484K
K417N N501Y
D614G
A701V
S1/S2
S2'
1
NTD
RBD
SD1
SD2
FP
HR1
HR2
TM
CTD
1273
14
306
331
528
591
686
816
834
910
985
1163
1211
S1
S2
B
N501Y
E484K
K417N
ΔL242-244
L18F
R246I
D80A
D215G
D614G
A701V
C
Database Mutation Frequency (%)
100
75
50
25
0
Dec Feb Apr Jun Aug Oct Dec Feb Apr
Mutations
ΔL242−244*
N501Y
D215G*
D614G
D80A*
E484K*
K417N*
L18F
A701V*
R246I*
D
417N
E
484K
F
501Y
G
1
10000
20000
30000
5'
3'
ORF1ab
s
3a
E
M
6
7a
7b
8
9b
N
G174T
C26456T
C26645T
T27504C
C28887T
1 2 3 4 5 6 7 8 9 10 12 13 14 15 16
C1059T
A2692T
G5230T
A10323G
C14925T
3a
G25563G C25904T
S
C21614T
A21801C
A22206G
Δ22286-22294
G22299T
G22813T
G23012A
A23063T
A23403G
C23664T

Figure 7

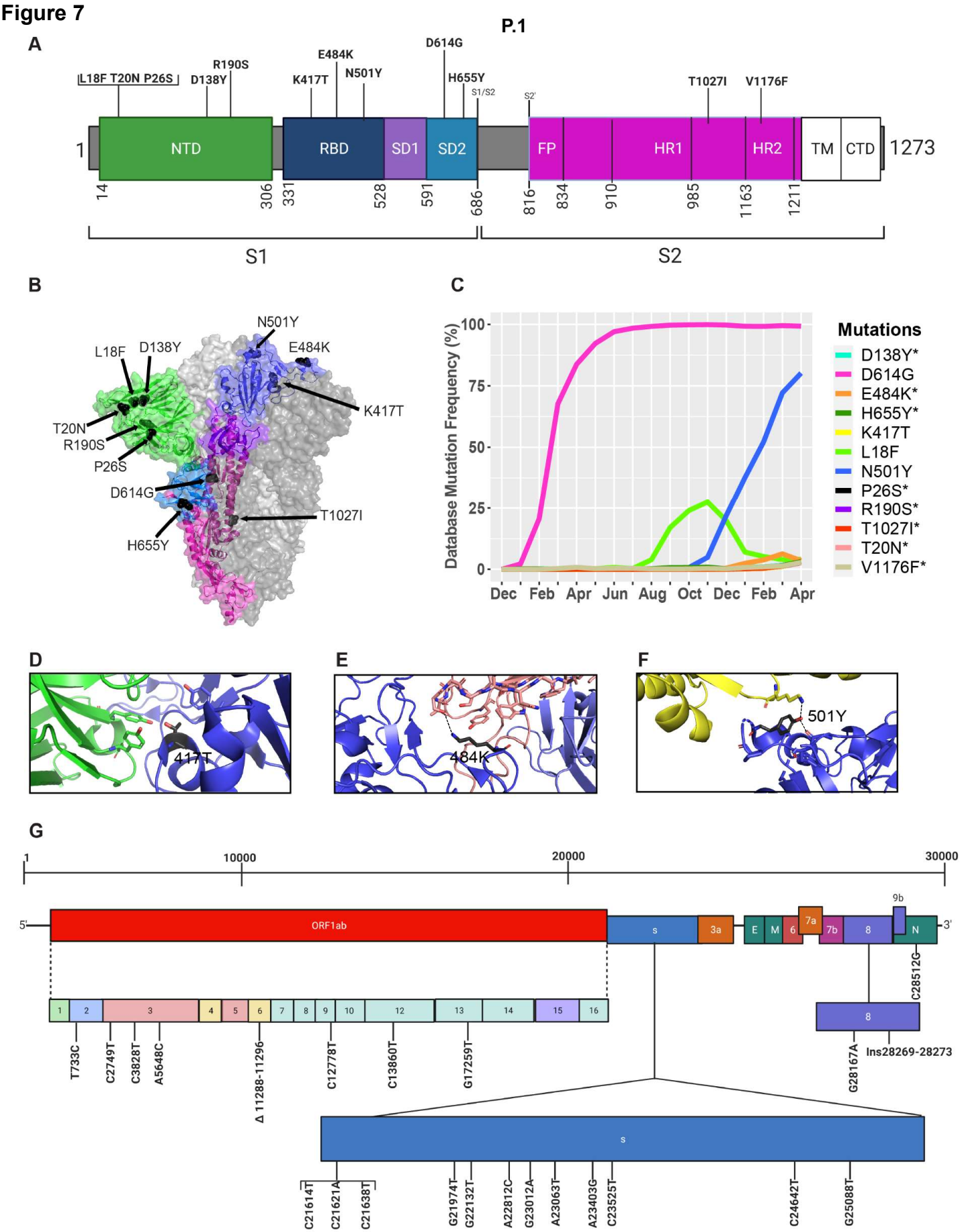
A
P.1
L18F T20N P26S
D138Y
R190S
K417T
E484K
N501Y
D614G
H655Y
S1/S2
S2'
T1027I
V1176F
1
NTD
RBD
SD1
SD2
FP
HR1
HR2
TM
CTD
1273
14
306
331
528
591
686
816
834
910
985
1163
1211
S1
S2
B
N501Y
L18F
D138Y
E484K
K417T
T20N
R190S
P26S
D614G
T1027I
H655Y
C
Database Mutation Frequency (%)
100
75
50
25
0
Dec
Feb
Apr
Jun
Aug
Oct
Dec
Feb
Apr
Mutations
D138Y*
D614G
E484K*
H655Y*
K417T
L18F
N501Y
P26S*
R190S*
T1027I*
T20N*
V1176F*
D
417T
E
484K
F
501Y
G
1
10000
20000
30000
5'
ORF1ab
s
3a
E
M
6
7a
7b
8
9b
N
3'
C28512G
1
2
3
4
5
6
7
8
9
10
12
13
14
15
16
T733C
C2749T
C3828T
A5648C
Δ 11288-11296
C12778T
C13860T
G17259T
G28167A
Ins28269-28273
C21614T
C21621A
C21638T
G21974T
G22132T
A22812C
G23012A
A23063T
A23403G
C23525T
C24642T
G25088T
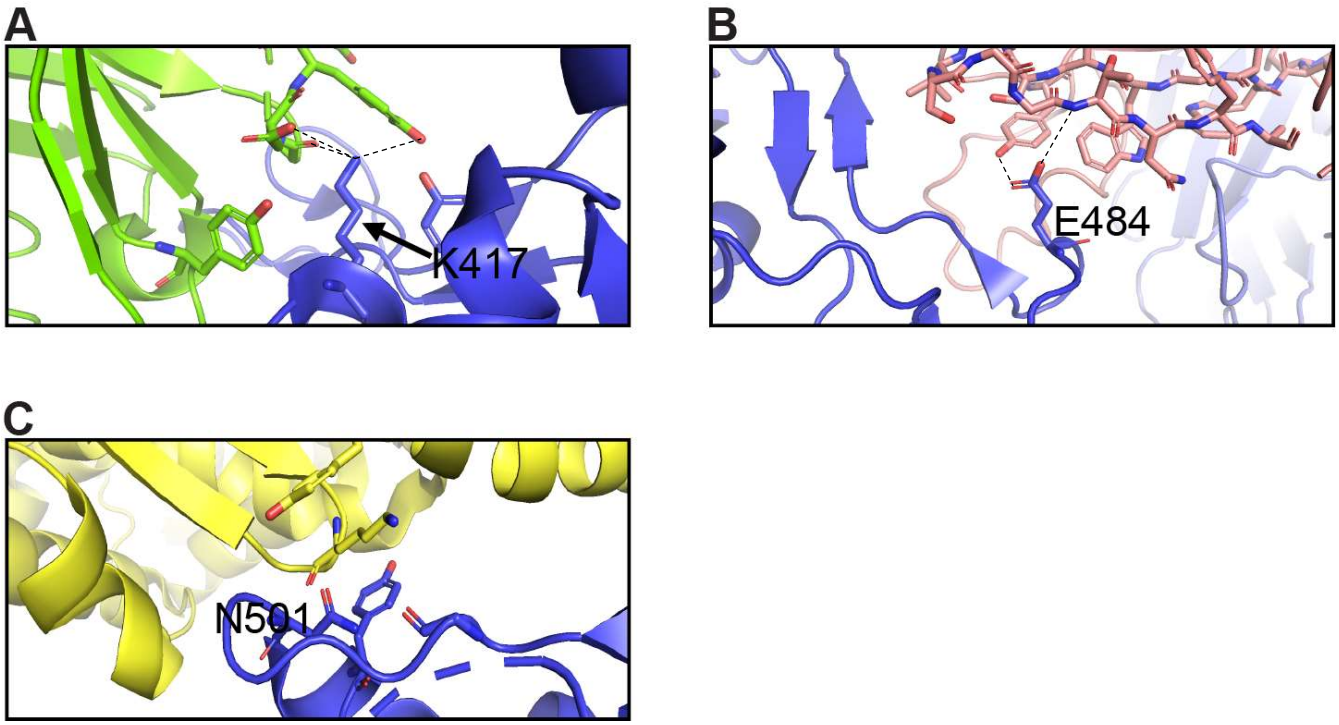
Figure 8